Decentralized Coefficient Diagram Method Based Robust Frequency Control Design in Power System

分散型係数図形法に基づく電力系統のロバスト周波数制御系設計

By

Michael Zontche Bernard
(Student ID: 12589504)

Supervisor: Prof. Yasunori Mitani, PhD.

Submitted in fulfillment of the requirements for the qualification

Doctor of Engineering Degree (D.Eng.) in Electrical Engineering

In the

Department of Electrical and Electronic Engineering
Graduate School of Engineering
Kyushu Institute of Technology

January 22, 2014

Dedicated to My God,

My Parents, My Wife Nathalia,

My Kids Archimedes and Karisma,

My Family, Friends and All Those Who

Take Pleasure in My Prosperity and Been

There for Me during the Times of Nonlinearities

Acknowledgements

To God the father of all, through Jesus Christ, I am thankful for the strength that keeps me standing and for the hope that keeps me believing that this research would be possible, more interesting and successful.

This project would not have been possible without the support of many people. First and foremost, I wish to express my sincere gratitude to my supervisor, Professor Yasunori Mitani who was very patient, abundantly helpful and tirelessly offered invaluable assistance, support and guidance. Without his knowledge and assistance this study would not have been successful. My deepest gratitude are also due to Prof. Masayuki Watanabe, Prof. Masayuki Hikita and Prof. Mochimitsu Komori, who served as my supervisory committee members, for their valuable suggestions, guidance and comments, during the period of my research.

I extend many thanks and appreciations to Dr. Yaser Qudaih and Dr. Tarek Mohammed for their technical guidance, thoughts and support during this research. All of my Japanese lab mates have always been there whenever I needed their assistance. My International students-friends of Mitani laboratory were also of great help towards my studies. To you my friends, I say many thanks for all your support during my five-and-the-half years at Kyushu Institute of Technology (KYUTECH).

I would also like to convey thanks to the Japanese government for the Monbukagakusho scholarship offered by the Ministry of Education, Culture, Sports, Science and Technology (MEXT), for providing the financial means. Many thanks also go to all members of the faculty and Administration of KYUTECH for all of the excellent classroom lectures, conducive learning environment and wonderful laboratory facilities.

My father Gaye Bernard and my mother Sarah Bernard have always encouraged me to seek answers to my many questions. I owe the curiosity that made me start this journey to them. In Japan, I found not only a friend but also a mother in Yoko Mori. She made me felt at home during my six years in japan and helped me to keep believing in God. Thank you Yoko Mori.

Life away from one's family isn't an easy task. Many thanks to my wife and kids for their patience and endless love. Thanks to the rest of my family members for love and support too.

I have discovered that I am a very rich man, though my banker would probably not agree. I have many good and close friends and that's a real fortune. I will not mention you by names (as there might not be enough space), but you know who you are. Thanks for being there for me when I needed you and thanks to all those who prayed for me.

Finally, I would like to thank Ms. Nagao and all the staffs of Student Affairs as well as the international student center. The secretaries of Mitani laboratory, Ms. Miki Tokumori and Ms. Aiko Toyoshima received acknowledgements for being my constant well-wishers.

Michael Zontche Bernard
January 2015

Abstract

In an interconnected power system, area load change and abnormal conditions leads to mismatches within the system. Also, in recent years, renewable energy systems (RES) such as Wind Energy Systems (WES) has become the most popular renewable energy based generations. However, output fluctuations of WES can create imbalance between supply and demand. This imbalance can cause network frequency variations in power systems and thus reduce the power quality.

To alleviate the mentioned problems, a control system is required to suppress the frequency fluctuations or oscillations caused by integrations of renewable energy sources and sudden load changes. Since, Proportional Integral (PI) controller cannot work under certain operating conditions, and due to problems of calculation burdens associated with the algorithms of other advance robust controllers such as Model Predictive Control (MPC), it is necessary to implement a controller that is simple and reliable.

The standard Coefficient Diagram Method (CDM) developed by Professor Shunji Manabe has an advantage because it is simple and robust, and solves the problem of calculation burden associated with MPC. But when the CDM is implemented for power system control, then problem of parameters' tuning exist. One important aspect of the CDM is the stability indices. When using CDM for power system frequency control, the standard values for the stability indices cannot work. Therefore, they must be changed. However, changing the stability indices can be done based on experience or by trial and error; and this becomes a problem for new power system control designers. Hence, this work modifies the standard CDM by introducing feed forward and feedback compensators to compensate for deficient performances. The technique is proposed as a new frequency control scheme using the Coefficient Diagram Method as a decentralized robust controller, in various test scenarios; considering varieties of power system configurations.

A three area interconnected power system is modelled, and this power system is assumed to be similar to the upcoming power system approved by the African development bank; which will interconnect Liberia, Guinea and Sierra Leone. These countries utilize hydro and steam turbines within their respective areas, but the problem of poor power quality which is highly related to frequency control requires attention. In this work, it is assumed that each country represents one area. Then, a three area power system assumed similar to their interconnection is modelled. With that, the proposed CDM is then implemented as control strategy to promote reliable electric power distributions.

Digital simulations of various case studies are provided to validate the effectiveness of the proposed scheme. From the simulation results, it is shown that, considering the overall closed-loop system performance with the proposed CDM technique, robustness is demonstrated in the face of uncertainties due to governors and turbines parameters variation and loads disturbances. A performance comparison between the proposed controller, model predictive controllers (MPC), and a classical proportional integral control (PI) scheme is carried out, confirming the superiority of the proposed CDM technique.

Table of Contents

List of Figures

List of Tables

List of Acronyms

AC – Alternative Current
AFDB – African Development Bank
ANN–Artificial Neural Network
AVR – Automatic Voltage Regulator
CDM–Coefficient Diagram Method
CR– Customer Requirement
DC– Direct Current
DEG. –Degree
DFIG – Doubly Fed Induction Generator
DQ – Direct and Quadrature
ECC – Energy Control Centers
FOC – Field Oriented Control
GA– Genetic Algorithm
GALMI–Genetic Algorithm and Linear Matrix Inequalities
GOL–Government of Liberia
GPC – Generalized Predictive Control
GRC – Generation Rate Constraint
HAWT – Horizontal Axis Wind Turbine
HDVC–High Voltage Direct Current
KYUTECH – Kyushu Institute of Technology
LEC – Liberia Electricity Corporation
LFC – Load Frequency Control
MRU – Mano River Union
MPC – Model Predictive Control
MV – Manipulated Variables
PD – Proportional Derivative
PEC – Power Electronic Converter
PG – Generated Power
PI – Proportional Integral
PID – Proportional Integral Derivative
PM – Permanent Magnet
PWM – Pulse Width Modulation
PV–Photovoltaic
REA – Rural Electric Administration
RES-Renewable Energy System
TSR – Tip Speed Ratio
VAWT – Vertical Axis Wind Turbine
VSC – Voltage Source Converter
VSWT – Variable Speed Wind Turbine
WECS – Wind Energy Conversion System
WT – Wind Turbine

Chapter 1

Introduction

1.1 Research Problems and Motivation

The world has become more and more dependent on electricity. For this reason, the demand in the production of electric power increases. Hence, power system continues to evolve and becomes more and more complex with respect to the developmental growth in its size and scale. As the complexity of electric power system increases, reliability becomes a vital issue; and to obtain this, large-scale interconnected power systems are utilized. The use of large-scale power interconnected power system is intended to make electric power generation and transmission more economical and reliable.

However, in an interconnected power system, sudden area load changes and abnormal conditions such as varying system parameters may cause mismatches in frequency, and scheduled tie-line power flows between areas. In terms of these abnormal conditions, the frequency falls, and this causes the turbine regulating devices to fully open and the generating units becomes completely loaded. As the frequency decreases, the generator exciter loses their speed and generator electromotive force (emf) falls and the voltage in the power system unit also drop. This brings the danger of a “voltage avalanche”, causing the interconnected power system to lose synchronism and consequently damage of equipment, and cascading blackouts or disconnection of the consumers [1].

On the other hand, the reduction of economic dependency on fossil fuel-based energy has been among the top priority goals of regulators and governments around the world. In recent years, fossil fuel resources are limited and have a significant adverse impact on the environment by raising the level of carbon dioxide (CO_2) in the atmosphere and contributing to global warming. Therefore, renewable energy systems (RES) such as wind energy conversion systems (WECS), solar energy or photovoltaic (PV) etc. are being integrated into power systems.

Wind energy system is the fastest growing renewable energy resource. But the wind is not stable. Therefore when it is integrated into power system, output fluctuations of wind generators can cause network frequency variations problems, which can consequently decrease the power quality [2].

To alleviate the above mentioned problems, a control system is required to suppress the frequency fluctuations and/or oscillations caused by integrations of renewable energy sources and other abnormal conditions like faults and sudden load changes.

Today, control system designers are trying to apply different control algorithms in order to find the best controller parameters to obtain optimum solutions. Fixed parameter controllers, such as an integral controller or proportional integral (PI) controller, is widely employed in frequency control application or Load frequency control (LFC). However, there are two most important performance criteria that these controllers should meet-and they are, the reference tracking and the disturbance rejection regulation. For fix parameter controllers, the problem is that optimal tuning for one requirement may not give satisfactory performance for the other requirement. As a result, fixed parameter controllers which are only designed at nominal operating points, may no longer be suitable to work in all operating conditions.

For this reason, adaptive gain scheduling approaches have been proposed for LFC synthesis [3]. This method overcomes the disadvantages of the conventional Proportional Integral and Derivative (PID) controllers which need adaptation of controller parameters. However, it faces some disadvantages such as the instability of transient response as a result of abrupt changes in the system parameters coupled with the difficulties of obtaining accurate linear time invariant models at variable operating points [3].

In addition to dealing with changes in system parameters, intelligent methods have been introduced in many reports for LFC design. The application of fuzzy logic controllers have been used in a two area power system in [4, 5]. Other intelligent methods such as the applications of artificial neural network (ANN) and genetic algorithms (GA) in LFC have been reported in [6, 7]. Although intelligent methods gives promising results wherein parameters' estimation is not required and the parameters of the controllers can be changed generally very quickly. Moreover, their control algorithms are too complicated and unstable transient response could still be observed; therefore, some other elegant techniques are needed to achieve a more desirable performance.

Recently, some papers have reported the application of robust control schemes such as model predictive control (MPC) technique on load frequency control issues [8, 9]. In [8], the use of MPC in a multi area power system is discussed. In [9], the effect of merging wind turbines on a multi area power system controlled by MPC is discussed. From [8] and [9], fast response and robustness against parameter uncertainties and load changes can be obtained using MPC controller. On the other hand, positive effect of wind turbines (WTs) was observed. Though MPC showed good dynamic response, the algorithms associated with MPC are also complicated. Hence, problems of calculations burden remains an obstacle in the way of real time implementation of MPC. Due to increase in the complexity and change of the power system structure, other techniques are still needed to achieve a desirable performance.

The standard Coefficient Diagram Method (CDM) developed by Professor Shunji Manabe has the advantage because it is simple and robust, and solves the problem of calculation burden associated with MPC [10]. Nevertheless, when the CDM is implemented for power system control, problems of parameters' tuning become an issue. This is because power system is very large, the structure of power system is changing time by time and the complexity of power system is always increasing. Therefore, the tuning of CDM parameters for power system frequency control becomes a problem. One important aspect of the CDM is the stability indices. However, when using CDM for power system frequency control, then the standard values for the stability indices cannot work. Hence, these standard stability indices must be changed. Changing the stability indices can be done based on experience or by trial and error; and this becomes a problem for new power system control designers. Considering the above problems, with the aim of controlling large systems such as interconnected power systems using the CDM technique, modification or improvement of the standard CDM controller is required in order to design the controller to meet tracking and regulation characteristics.

This work therefore modifies the standard CDM by introducing feedforward and feedback compensators to compensate for deficient performances. The technique is proposed as a new frequency control scheme using the Coefficient Diagram Method as a decentralized robust controller, in various test scenarios considering varieties of power system configurations.

A three area interconnected power system is modeled, and this power system is assumed to be similar to the approved upcoming power system which will interconnect Liberia, Guinea and Sierra Leone. These three countries utilize hydro and steam turbines within their respective areas but the problem of poor power quality which is highly related to frequency control requires attention. To solve this problem, the African development Bank (AFDB) has approved a project to interconnect the power system of these countries so as to ensure reliability. Although, the date of implementation of the project is unknown and beyond the scope of this work, this research considers an assumption that each country represents one control area. Then after modeling a three area power system similar to their interconnection, the proposed CDM is implemented as control strategy to promote reliable power distributions.

The work is written in the form of papers, which were presented at conference proceedings and published in technical journals.

1.2 Research OBJECTIVE

The study accomplished the following objectives:

- Developed a decentralized robust frequency controller that is simple and reliable for large power system.
- Designed, introduced and implemented the CDM as a standalone decentralized frequency controller for frequency control of large power systems; and evaluated the proposed CDM controller for robustness and reduction of the effect of uncertainties owing to variations in the parameters of governors and turbines as well as load disturbance
- Modifies the standard CDM by introducing and implementing feed forward and feedback compensators so as to effectively employ the parameters of the proposed controller. The compensators can also cause an exchange in signals from outside of the feedback-loops which can ensure the overall stability of the power system. The feed forward compensator has an influence on the system from the reference input to the output and can be used to increase the speed of the transient response without affecting the transfer function from the disturbances to the output.
- Introduced and analysed an assumed frequency response model of interconnected power system of Liberia, Guinea and Sierra Leone, considering physical constraints of governors and turbines; and implemented the CDM as a frequency controller in the assumed power system.
- Investigated the effectiveness of the proposed control scheme in both interconnected power system and single area power system with wind farm integration in regards to its contribution in damping of power system frequency oscillations during sudden load change, and smoothing of frequency variations caused by changed in wind speed.
- Verify through digital simulations that the developed control scheme is more effective for enhancement of frequency quality and power system reliability as compared to MPC or conventional PI controller

1.3 Thesis Outline

The rest of the thesis is structured as follows:

Chapter 2: Discusses frequency control in power system and with main emphasis on PID and MPC. An overview of PID controller is carried out and the general consideration about MPC and its cost function are discussed.

Chapter 3: Provides a general consideration about CDM and its design. The introduction and implementation of feed forward and feedback compensators for the proposed CDM are presented.

Chapter 4: Considers the first case study involving CDM application to multi-area interconnected power system. The interconnected power system assumed similar to the approved power system which will interconnect Liberia, Guinea and Sierra Leone is discussed and modeled. The system dynamics and overall system structure are presented with the proposed CDM controller.

Chapter 5: Deals with the Integration of wind farm into power grid. The impact of wind power on power system dynamics is studied. Problems involving voltage and frequency are highlighted.

Chapter 6: Deals with the second case study which involves smoothing of output fluctuations caused by the integration of wind farm. A single area power system is modelled and the power system is assumed similar to Liberia power system and integration of wind turbines into the power system is considered. Then the implementation of the proposed CDM to solve the problem of output fluctuations is highlighted.

Chapter 7: Concludes the thesis

1.4 References

[1] Ajitha priyadarsini .S, P. Melba Mary.” Load Frequency Control in Co-ordination with Frequency Controlable HDVC Links Using Fuzzy Logic Controllers” International Journal of Research in Engineering and Technology eISSN: 2319-1163 | pISSN: 2321-7308

[2] H. Bevrani, "Robust Power system control", Springer, New York, 2009.

[3]Talaq J, Al-Basri F. Adaptive fuzzy gain scheduling for load frequency control.

IEEE Trans Power Syst 1999; 14(1):145–50.

[4] HO Jae Lee, Jin Bae Park, Young Hoon Joo, Robust LFC for Uncertain nonlinear power systems: a fuzzy logic approach. Inform Sci 2006; 176:3520–37.

[5] Cam E, Kocaarslan I. Load frequency control in two area power systems using fuzzy logic controller. Energy Convers Manage 2005; 46:233–43.

[6] Birch AP, Sapeluk AT, Ozveren CS. An enhanced neural network load frequency control technique. ASCE J 2005;5(II) [Control 94, 21–24 March 1994, Conference Publication No. 389, IEE 1994]

[7] Abdel-Magid, Y. L. and Dawoud, M. M., "Genetic Algorithms Applications In Load Frequency Control", Genetic algorithms in engineering systems: innovations and applications, 12-14 September 1995, conference publications No. 414, IEE, 1995.

[8] T. H. Mohamed, H. Bevrani, A. A. Hassan, T. Hiyama. Decentralized model predictive based load frequency control in an interconnected power system. Energy Convers Manage 2011; 52:1208–41.

[9] Michael Z. Bernard, T.H.Mohammed, Yasunori Mitani, Yaser Soliman Qudaih. “CDM Application in Power System as a Load Frequency Controller.” Proceedings of the 13th annual Electrical Power and Energy Conference (EPEC 2013), Halifax, Nova Scotia, Canada

Chapter 2

Frequency Control in Power System

2.1 Introduction

For the all-round development of any country and industrial development, Electrical power plays a significant role. It generates and distributes electrical power to factories and households, to meet varieties of power needs. During the generation and distribution process, both the active power balance and reactive power balance must be maintained between generation and utilization of the electric power. Those two balances correspond to two equilibrium points which are frequency and voltage. When either of the two balances is broken and reset at a new level, the equilibrium points will float. Although active power and reactive power affect the frequency and voltage respectively, the frequency is highly dependent on the active power while the voltage is highly dependent on the reactive power. Hence, the control issue in power systems can be decoupled into two independent problems. One is about the active power and frequency control while the other is about the reactive power and voltage control. The active power and frequency control is referred to as load frequency control (LFC) [1] or simply frequency control which is the major concerned of this thesis.

One important goal of LFC is reliability and this is concerned with obtaining good electric power quality. To achieve reliable electric power, the frequency must remain at standard value during operations. Hence, large-scale interconnection power systems are often utilized. The interconnection is intended to make the electrical power generation and transmission more economical and reliable. In modern large interconnected power systems, controllers are set for a particular operating condition and they are important to cancel or reduce the effect of random or sudden changes in load demand and keeping the frequency and voltage at standard values.

An interconnected power system consists of number of areas. These areas are interconnected by means of AC tie-lines or HVDC transmission links. It is necessary to maintain the constant frequency so that the power stations run satisfactorily in parallel and various motors operating in the system run at the desired speed. By implementing effective control strategy to achieve a balance between the generation and the connection of load, the frequency can be made stable to a major extent [3].

If the frequency is not properly control and kept within permissible limits, the generator exciter loses their speed, the generator emf falls and causes the voltage in the power system unit to drop which seriously leads to disconnection of consumers. Therefore,

frequency control is very important in power system operation and security for supplying sufficient and reliable electric power with good quality.

It has already been stated earlier that real and reactive powers are controlled separately because changes in real power affect mainly the system frequency while reactive power is less sensitive to changes in frequency and is mainly dependent on changes in voltage magnitude. Thus, LFC loop controls the real power and frequency while automatic voltage regulator (AVR) loop regulates the reactive power and voltage magnitude.

LFC has gained in importance with the growth of interconnected systems. It has made the operation of interconnected systems possible [4] and even up to today, it is still the basis of many advanced concepts for the control of large systems. The methods was developed for control of individual generators, and eventually control of large interconnections, and play a vital role in modem energy control centers (ECC). This chapter deals with the frequency control of power system so as to understand the concept of maintaining steady-state. In addition, simple models of the essential components used in control systems are presented and a general overview of Model predictive Control MPC and PID controllers is carried out

2.1.1 Factors that Affects Power System Frequency

Several factors may cause problems in power system frequency. Some of these issues are sudden area load changes, network frequency variations due to integration of renewable energy systems (RES) [for example: Wind Energy Systems (WES), Solar Power or PV etc.], and abnormal conditions, such as outages of generation, faults on transmission lines and varying system parameters. These issues can cause mismatches in frequency and scheduled tie-line power flows between areas. The main requirement of frequency control is to correct those mismatches by ensuring that the frequency of the power system is maintained at or near specified nominal value, and also to ensure that the tie-line power flows among the interconnection areas are maintained at specified levels [4,].

2.2 Existing Frequency Control Solutions

There is no exact amount of solutions for frequency control. As technology advances, new solutions are being developed while classical methods are being improved. This section points out some famous LFC techniques.

Conventional Control (Proportional Integral control)–In industry, proportional-integral (PI) controllers have been broadly used for decades as the load frequency controllers. A PI controller design on a three-area interconnected power plant is presented in [5], where the controller parameters of the PI controller are tuned using trial-and-error approach.

Fuzzy logic control–This method is based on fuzzy set theory, in which the fuzzy logic variables can be any value between 0 and 1 in contrast to classical or digital logic, which operates on discrete values of either 1 or 0 (true or false, respectively). Decision is made through fuzzy logic functions after the variables are selected. Application of Fuzzy Logic has been applied in several research for decentralized LFC problem [6-8], tie line bias control scheme [7] , and fuzzy gain scheduled PI control scheme [8] etc.

Genetic algorithm (GA)–is effective in solving complex optimization problems. In [9] PI-type controllers tuned via GA and linear matrix inequalities (GALMI) is presented on a decentralized three-area nine-unit power system. Results show that the structure of the GALMI tuned PI controller is simpler than that of the H2/H-infinity (H_2/H_∞) controller although the performances of the two methods are equivalent.

Model Predictive Control (MPC)–has proved an efficient control in a wide range of applications in industries. The MPC scheme is based on an explicit use of a prediction model of the system response to obtain the control actions by minimizing an objective function. In other words, MPC uses the current plant measurements, the current dynamic state of the process, the MPC models, and the process variable targets and limits to calculate future changes in the dependent variables. The models used in MPC are generally intended to represent the behavior of complex dynamical systems. However, the additional complexity of the MPC control algorithm is not generally needed to provide adequate control of simple systems, which are often controlled well by generic PID controllers. The MPC has proven to be robust by demonstrating fast response and robustness against parameter uncertainties and load changes in [10].

2.2.1 Centralized and Decentralized Frequency Control

LFC design carried out on an entire power system model without considering subsystems is known as centralized method. Some researches has used centralized method [11] and [12] with a simplified multiple-area power plant in order to implement some optimization techniques on the entire model. However, the simplification is based on the assumption that all the subsystems of the entire power system are identical while they are not. The assumption makes the simulation model in the paper quite different from the real system. Another problem for the centralized methods is

that even if the method works well on a low-order test system, it would face an exponentially increasing computation problem with the increase of the system size.

Since the tie-line interfaces give rise to weakly coupled terms between areas, the large-scale power system can be decentralized into small subsystems through treating tie-line signals as disturbances. Numerous control techniques have been applied to the decentralized power systems [13]. Since H_2/H_∞ control is well known for its robustness against parameter uncertainties, the controller has been utilized to solve the decentralized LFC problems in [14]. There are also several other modern control theories that have used decentralized solutions of LFC problem, such as disturbance accommodation control, optimal tracking approach, predictive control scheme and ramp following control, which can be found in [15].

Most of the reported solutions of LFC problems have been tested for their robustness against large step load change. However, very few of the published researches dealt with parameter uncertainties. In [16], the authors set up a 15% floating rate for the parameters in one area and successfully controlled the system with an optimally tuned PID controller. Nevertheless, in reference [16], a lot of approximations and simplifications have been made during the modeling process of the power systems, on which the controller is designed. The simplified system model has deviated far from the real system. A control technique with a notable robustness against not only parameter uncertainties but also model uncertainties, and external load change will be preferred by the power industry.

2.3 CONTROL LOOPS

In an interconnected power system, load frequency control (LFC), and automatic voltage regulator (AVR) equipment are installed for each generator. Figure 2.1 represents the schematic diagram of the load frequency control (LFC) loop and an automatic voltage regulator (AVR) loop. The controllers are set for a particular operating condition and take care of small changes in load demand in order to maintain the frequency and voltage magnitude within the specified limits. Small changes in real power are mainly dependent on changes in rotor angle δ and, thus, the frequency.

The reactive power is mainly dependent on the voltage magnitude (i.e. on the generator excitation). The excitation system time constant is much smaller than the prime mover time constant and its transient decay much faster and does not affect the

LFC dynamic. Thus, the cross-coupling between the LFC loop and the AVR loop is negligible. Therefore, the load frequency and excitation voltage control are analyzed independently. Voltage control is beyond the scope of this research and therefore, this work will be concern with only frequency control.

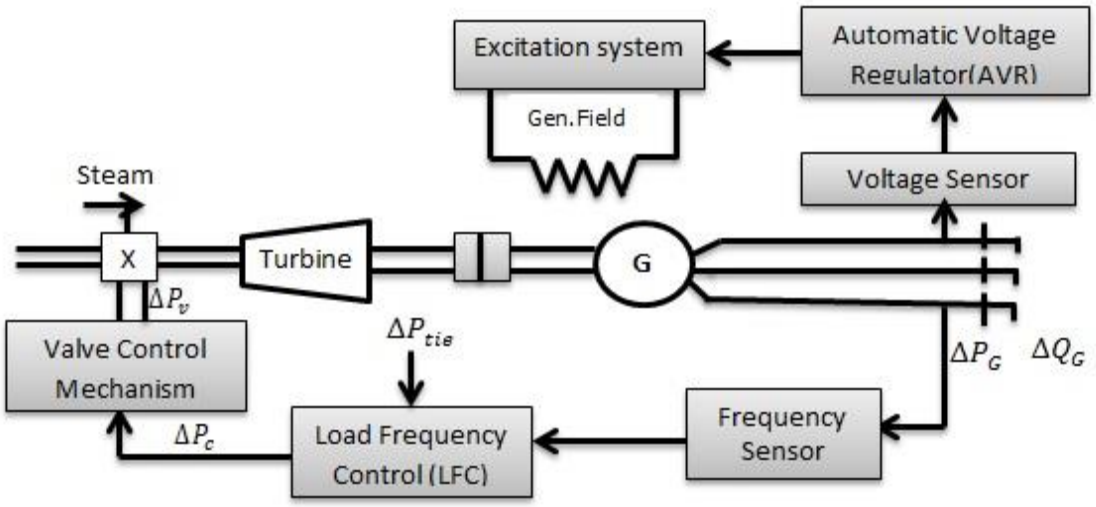

Figure 2.1. Schematic diagram of LFC and AVR of synchronous generator [4]

2.4 LOAD FREQUENCY CONTROL and Modelling

The operation objectives of the LFC are to maintain reasonably uniform frequency, to divide the load between generators, and to control the tie-line interchange schedules. The change in frequency which is a measure of the change in rotor angle δ, i.e., the error $\Delta\delta$ to be corrected, and tie-line real power are sensed. The error signal i.e., Δf and ΔP_{tie}, are amplified, mixed, and transformed into a real power command signal ΔP_v, which is sent to the prime mover to call for an increment the torque[4].

The prime mover, therefore, brings change in the generator output by an amount ΔP_g which will change the values Δf and ΔP_{tie} within the specified tolerance. The first step in the analysis and design of a control system is mathematical modeling of the system. The two most common methods are the transfer function method and the state variable approach. The state variable approach can be applied to portray linear as well as nonlinear systems. In order to use the transfer function and linear state equations, the system must first be linearized. Proper assumptions and

approximations are made to linearize the mathematical equations describing the system, and a transfer function model is obtained for the components such as the GENERATOR MODEL, LOAD MODEL, PRIME MOVER MODEL and GOVERNOR MODELS[4].

2.4.1 GENERATOR MODEL for LFC

Applying the swing equation of a synchronous machine to small perturbation, we have equation

$$\frac{1}{\omega_0}\frac{d\omega_r}{dt^2} = \Delta P_m - \Delta P_e \qquad (2.1)$$

or in terms of small deviation in speed

$$\frac{d\Delta\frac{\omega}{\omega_s}}{dt} = \frac{1}{2H}(\Delta P_m - \Delta P_e\ ) \qquad (2.2)$$

With speed expressed in per unit, without explicit per unit notation

$$\frac{d\omega}{dt} = \frac{1}{2H}(\Delta P_m - \Delta P_e\ ) \qquad (2.3)$$

Taking Laplace transform of (2.3) yields

$$\Delta\omega(s) = \frac{1}{2H_s}[\Delta P_m(s) - \Delta P_e(s)\ ] \qquad (2.4)$$

The above relation is shown in block diagram formed in Figure 2.2.

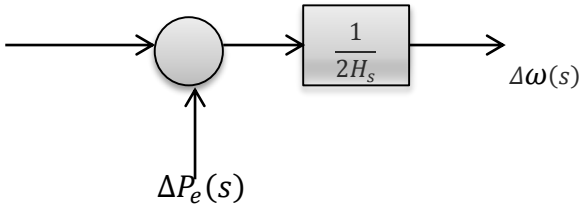

Figure 2.2. Generator block diagram

2.4.2 LOAD MODEL

The load on a power system consists of a variety of electrical devices. In order to model the load, it is important to know that some loads are frequency-sensitive while others are not. The frequency-sensitive loads, such as motor loads are sensitive to changes in the frequency. For resistive loads, such as lighting and heating loads, the electrical power is independent of frequency. How sensitive the frequency-sensitive loads are to frequency depends on the composite of the speed-load characteristics of all the driven devices. The speed-load characteristic of a composite load is the sum of resistive load ΔP_L and frequency-sensitive load $D\Delta\omega$ and is approximated by

$$\Delta P_e = \Delta P_L + D\Delta\omega \qquad (2.5)$$

D is expressed as percent change in load divided by percent change in frequency. For example, if load is changed by 2.5 percent for a 1 percent change in frequency, then *D = 2.5*.

Now the goal is to include a load in the generator model of equation 2.4 because the generator must supply a load. According to equation 2.4, the generator model is given by

$$\Delta\omega(s) = \frac{1}{2H_s}[\Delta P_m - \Delta P_e\ ] \qquad (2.5a)$$

Hence, if $\Delta P_L + D\Delta\omega$ from the load model of equation 2,5 is substituted for ΔP_e in the generator model of equation 2.4 or 2.5a, then

$$\Delta\omega(s) = \frac{1}{2H_s}[\Delta P_m - (\Delta P_L + D\Delta\omega(s)\ )\ ] \qquad (2.6)$$

Hence collecting like terms and simplifying equation (2.6) gives

$$\Delta\omega(s) = \frac{1}{2H_s + D}[\Delta P_m - \Delta P_L] \qquad (2.7)$$

Equation 2.7 shows the load model included in the generator model and the block diagram is displayed in Figure 2.3 below.

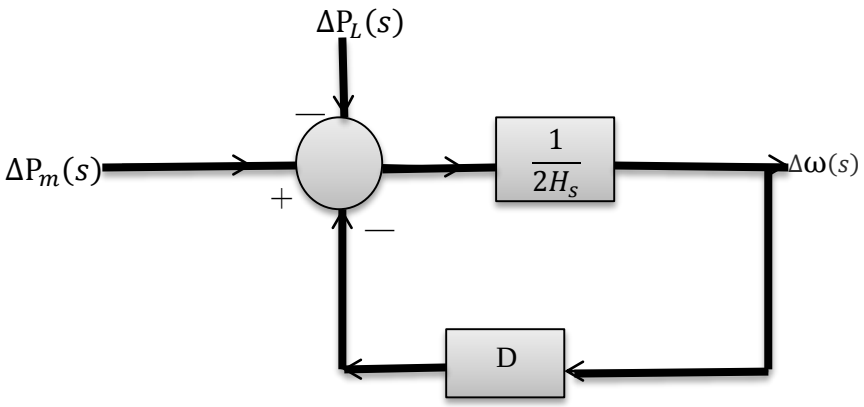

Figure 2.3. Generator and load block diagram

In order to eliminate the feedback loop, block diagram transformation theorem is applied [18]. From the concept of block diagram algebra it is know that

$$\frac{C}{R} = \frac{G}{1+GH} \qquad (2.8)$$

Where G is the direct transfer function, H is the feedback transfer function and GH is the loop transfer function or open loop transfer function. In this case, the output, C, is $\Delta\omega(s)$ and the input is R, is $\Delta P_m - \Delta P_L$. Also, $= \frac{1}{2H_s}$, while $H = D$.Therefore equation 2.8 can be re-written as

$$\frac{\Delta\omega(s)}{\Delta P_m - \Delta P_L} = \frac{\frac{1}{2H_s}}{1 + (\frac{1}{2H_s})(D)} \qquad (2.8a)$$

Simplifying equation 2.8a leads back to equation 2.7. Thus when the feedback loop is eliminated, figure 2.3, results actually in the block diagram shown in Figure 2.4.

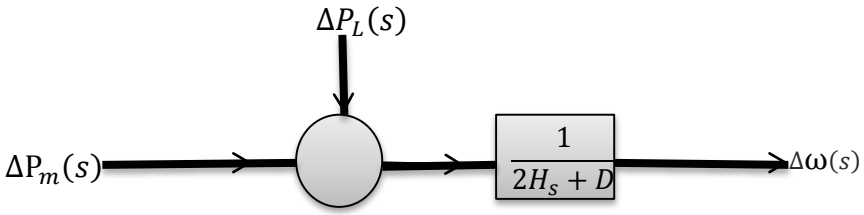

Figure 2.4. Generator and load block diagram with feedback loop eliminated

2.4.3 PRIME MOVER MODEL

The source of mechanical power is commonly known as the prime mover. The prime mover may be hydraulic turbines at waterfalls, steam turbines whose energy comes from the burning of coal, gas, nuclear fuel, and gas turbines. The model for the turbine relates changes in mechanical power output ΔP_m to changes in steam valve position, ΔP_V. Different types of turbines vary widely in characteristics. The simplest prime mover model for the non-reheat steam turbine can be approximated with a single time constant T_T, resulting in the following transfer function

$$G_T(s) = \frac{\Delta P_m(s)}{\Delta P_V(s)} = \frac{1}{1 + T_{Ts}} \qquad (2.6)$$

The block diagram for a simple turbine is shown in Figure 2.5 below.

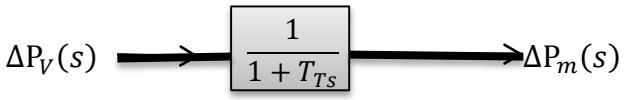

Figure 2.5. Block diagram of simple non-reheat steam turbine

It is important to know that the time constant T_{Ts} is in the range of 0.2 to 2.0 seconds.

2.4.4 GOVERNOR MODEL

When the generator electrical load is suddenly increased, the electrical power exceeds the mechanical power input. This power deficiency is supplied by the kinetic energy stored in the rotating system. The reduction in kinetic energy causes the turbine speed and, consequently, the generator frequency to fall. The change in speed is sensed by the turbine governor which acts to adjust the turbine input valve to change the mechanical power output to bring the speed to a new steady state. The earliest governors were the Watt governors which sense the speed by means of rotating flyballs and provide mechanical motion in response to speed changes. However, most modem governors use electronic means to sense speed changes. The conventional Watt governor consists of the following major parts:

I. Speed Governor: The essential parts are centrifugal flyballs driven directly or

through gearing by the turbine shaft. The mechanism provides upward and downward vertical movements proportional to the change in speed.

2. Linkage Mechanism: These are links for transforming the flyballs movement to the turbine valve through a hydraulic amplifier and providing a feedback from the turbine valve movement.

3. Hydraulic Amplifier: Very large mechanical forces are needed to operate the steam valve. Therefore, the governor movements are transformed into high power forces via several stages of hydraulic amplifiers.

4. Speed Changer: The speed changer consists of a servomotor which can be operated manually or automatically for scheduling load at nominal frequency.

By adjusting the set point, a desired load dispatch can be scheduled at nominal frequency. For stable operation, the governors are designed to permit the speed to drop as the load is increased.
The steady-state characteristic of such a governor is shown in Figure 2.6 below (not drawn to scale).

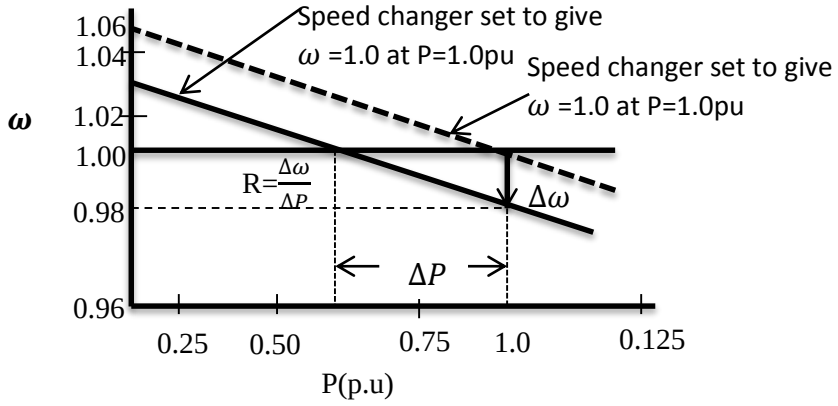

Figure 2.6. Governor Steady-State Characteristics

The slope of the curve represents the speed regulation R. Governors typically have a speed regulation of 5-6 percent from zero to full load. The speed governor mechanism acts as a comparator whose output ΔP_g is the difference between the reference set

power ΔP_{ref} and the power $\frac{1}{R}\Delta\omega$ as given from the governor speed characteristics. Hence,

$$\Delta P_g = \Delta P_{ref} - \frac{1}{R}\Delta\omega \qquad (2.7)$$

or in the s—domain ,

$$\Delta P_g(s) = \Delta P_{ref}(s) - \frac{1}{R}\Delta\omega(s) \qquad (2.8)$$

The command ΔP_g is transformed through the hydraulic amplifier to the steam valve position command ΔP_V. Assuming a linear relationship and considering a simple time constant T_g we have the following s-domain relation:

$$\Delta P_V(s) = \frac{1}{1+T_g}\Delta P_g(s) \qquad (2.9)$$

The block diagram for Equations (2.8) and (2.9) are represented by the block diagram shown in Figure 2.7 below.

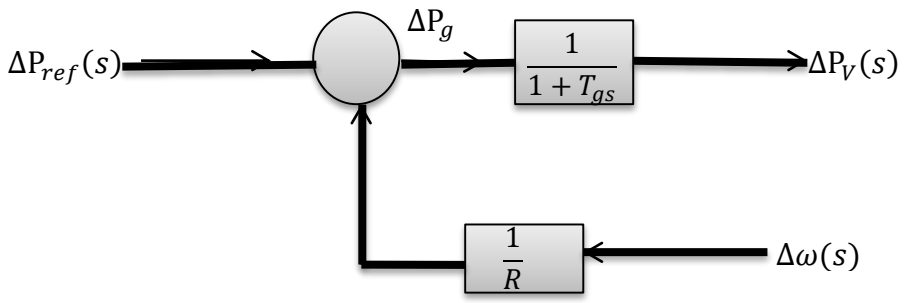

Figure 2.7. Block Diagram Representation of Speed Governor System for Steam Turbine

When the block diagrams of figures 2.4, 2.5, and 2.7 are combine, this results in the complete block diagram of the load frequency control of an isolated power system shown in figure 2.8.

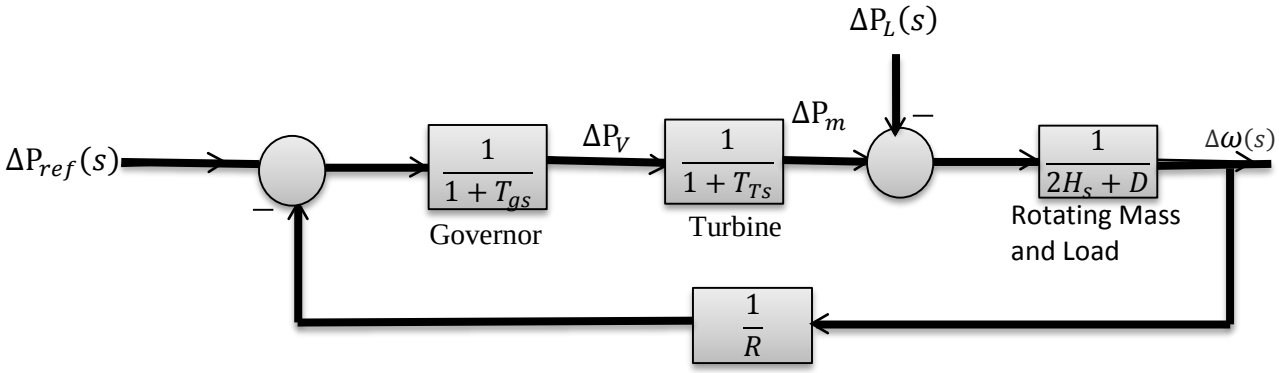

Figure 2.8. Load Frequency Control Block Diagram of an Isolated Power System

Redrawing the block diagram of figure 2.8 with the load change $\Delta P_L(s)$ as the input, and the frequency deviation $\Delta\omega(s)$ as the output, results in the block diagram shown in figure 2.9 below.

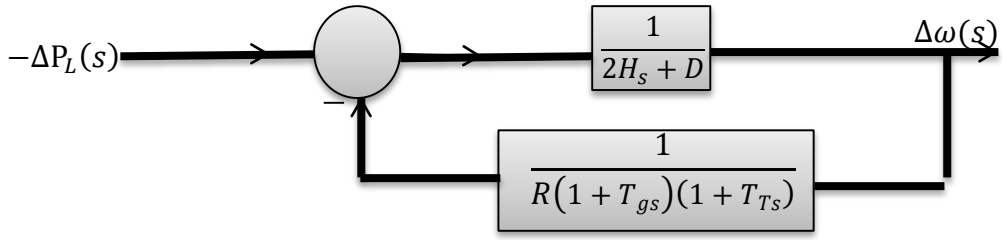

Figure 2.9. LFC block diagram with input $\Delta P_L(s)$ and output $\Delta\omega(s)$

The open-loop transfer function of Figure 2.9 is given by

$$KG(s)H(s) = \frac{1}{R}\frac{1}{(2H_s + D)(1 + T_{gs})(1 + T_{Ts})} \qquad (2.10)$$

It can be seen that the block diagram transformation theorem used in equations 2.8 and 2.8a respectively, can be applied to figure 2.9 so as to eliminate the feedback loop: $\frac{\Delta\omega(s)}{-\Delta P_L(s)} = \frac{\frac{1}{2H_S+D}}{\frac{1}{R(1+T_{gs})(1+T_{Ts})}}$ .Then when the result is simplified and both the numerator and denominator are divided by *R*, the closed-loop transfer function relating the load change $\Delta P_L(s)$ to the frequency deviation $\Delta\omega(s)$ is obtained. Thus,

$$\frac{\Delta\omega(s)}{-\Delta P_L(s)} = \frac{(1 + T_{gs})(1 + T_{Ts})}{(2H_s + D)(1 + T_{gs})(1 + T_{Ts}) + 1/R} \qquad (2.11)$$

Or

$$\Delta\omega(s) = -\Delta P_L(s)T(s) \qquad (2.12)$$

The load change is a step input, i.e., $\Delta P_L(s) = \Delta P_L/s$. Utilizing the final value theorem [4]. The steady-state value of $\Delta\omega$ is

$$\omega_{ss} = \lim_{s\to 0} s\Delta\omega(s) = (-\Delta P_L)\frac{1}{D + 1/R} \qquad (2.13)$$

It is clear that for the case with no frequency-sensitive load (i.e., with *D = 0*), the steady-state deviation in frequency is determined by the governor speed regulation:

$$\omega_{ss} = -\Delta P_L R \qquad (2.14)$$

So that for several generators with governor speed regulations $R_1, R_2 \ldots R_n$ are connected to the system, the steady-state deviation in frequency is given by

$$\omega_{ss} = (-\Delta P_L)\frac{1}{D + \frac{1}{R_1} + \frac{1}{R_2} + \cdots + \frac{1}{R_n}} \qquad (2.15)$$

Accurate frequency control in power system is essential. The primary reason for accurate frequency control is to allow the flow of alternating current power from multiple generators through the network to be controlled. There are several controllers that aid in controlling frequency. However, this chapter is only concern with two of them namely the Model Predictive Control (MPC) and the Proportional-Integral-Derivative (PID). Hence, in the next session an over view of PID and MPC is discussed.

2.5. Overview of PID controller

2.5.1 Preview

PID controller is a basic control prototype that uses the error, its time derivative, and its integral with respect to time to construct a signal that is used to drive the actuators. The actuators in turn affect the behavior of the process being controlled [15]. Figure 2.10 below shows a schematic diagram of a conventional PID controller.

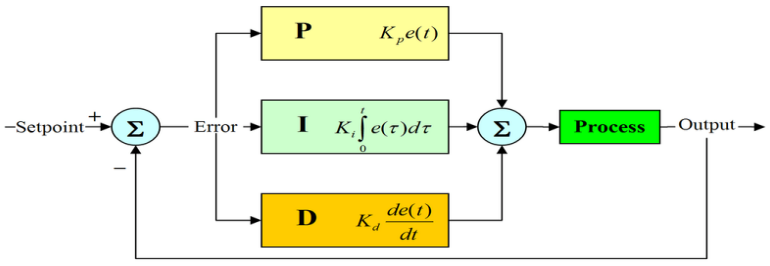

Figure 2.10. Diagram of PID Controller

A control signal that is proportional to the error cannot be expected to result in good damping and fast response and therefore may have unacceptable-steady state error. Introducing an integral term can eliminates steady-state errors but may adversely affect the damping. A term proportional to the derivative of the error can improve the speed of response and the damping, but it will not reduce steady-state errors. PID controllers provide significant improvements in response to time, damping, and steady-state error reduction.

In the PID control scheme, the sum of the *P*, *I* and *D* terms (the three correcting terms) constitutes the manipulated variable (MV). The proportional, integral, and derivative terms are summed to calculate the output of the PID controller.

2.5.2 The proportional Term

The proportional term makes the current error signal multiply with the proportional gain K_p to give the output signal. If the error function is represented by $e(t)$, and the output of the controller is $u(t)$, then

$$u(t) = K_p e(t) \qquad (2.16)$$

Hence, with a proportional controller offset (deviation from set-point) is present. Increasing the controller gain will make the loop go unstable. Integral action was included in controllers to eliminate this offset.

2.5.3 The Integral Term

The integral term makes the current error signal value and duration multiply with the gain K_i tp give the output. Therefore,

$$u(t) = K_i \int_0^t e(t)dt \qquad (2.17)$$

Where t is the instantaneous time and K_i is the integral gain. The integral of a signal is the sum of all the instantaneous values that the signal has been from the time you started counting to the time you stop counting. The integral term, when added to the proportional term, accelerates the movement of the process and eliminates the residual steady-state error that occurs with the proportional-only controller.

2.5.4 The Derivative Term

The derivative term makes the rate of change of the error signal multiplies with the gain $\mathrm{K_D}$ which is the derivative gain.

Thus,

$$u(t) = K_D \frac{d}{dt} e(t) \qquad (2.18)$$

Hence, the derivative term slows the rate of change of the control output and this effect is most noticeable closed to the controller set point. Combining the signals of the *P,I* and *D* terms of the PID controller above, The net controller output, which is the final form of the PID algorithm is:

$$u(t) = K_p e(t) + \ K_i \int_0^t e(t)dt + K_D \frac{d}{dt} e(t) \qquad (2.21)$$

PID controller will be called a *PI*, *PD*, *P* or *I* controller in the absence of the respective control actions. PI controllers are fairly common, since derivative action is sensitive to measurement noise, whereas the absence of an integral term may prevent the system from reaching its target value due to the control action. While PID controllers are applicable to many control problems, and often perform satisfactorily without any improvements or even tuning, they can perform poorly in some applications, and do not in general provide optimal control. The fundamental difficulty with PID control is that it is a feedback system, with constant parameters, and no direct knowledge of the process and thus, overall performance is reactive and a compromise. Eventhough PID control is the best controller with no model of the process [17], better overall system performance can be obtained by incorporating a model of the process. Hence, if a model of the process is incorporated, other control strategies prove effective. The next section discusses such control scheme.

2.6 Model Predictive Control

The MPC has proved an efficient control in a wide range of applications in industry such as chemical process, petrol industry, electromechanical systems and many other applications. Figure 2.11 below illustrates a Simple structure of MPC controller .The MPC scheme is based on an explicit use of a prediction model of the system response

to obtain the control actions by minimizing an objective function. Optimization objectives include minimization of the difference between the predicted and reference response, and the control effort subjected to prescribed constraints. The effectiveness of the MPC is demonstrated to be equivalent to the optimal control. It displays its main strength in its computational expediency, real-time applications, intrinsic compensation for time delays, treatment of constraints, and potential for future extensions of the methodology. At each control interval, the first input in the optimal sequence is sent into the plant, and the entire calculation is repeated at subsequent control intervals. The purpose of taking new measurements at each time step is to compensate for unmeasured disturbances and model inaccuracy, both of which cause the system output to be different from the one predicted by the model [17]. An internal model is used to predict the future plant outputs based on the past and current values of the inputs and outputs and on the proposed optimal future control actions.

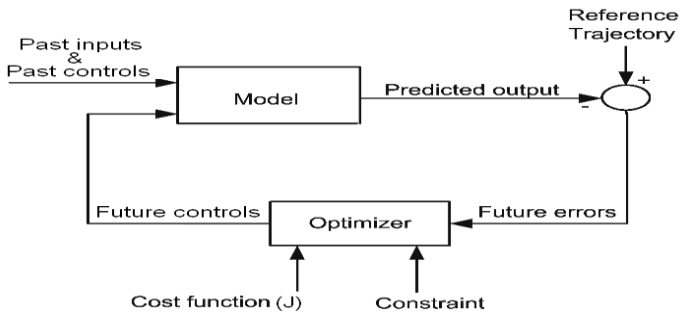

Figure 2.11. Simple Structure of MPC

The prediction has two main components : the free response which being expected behavior of the output assuming zero future control actions, and the forced response which being the additional component of the output response due to the candidate set of future controls. For a linear system, the total prediction can be calculated by summing both of free and forced responses. The reference trajectory signal is the target values the output should attain. The optimizer is used to calculate the best set of future control action by minimizing a cost function *(J)*. The optimization is subject to constraints on both manipulated and controlled variables .The general object is to tighten the future output error to zero, with minimum input effort. The cost function to be minimized is generally a weighted sum of square predicted errors and square future control values.

In Generalized Predictive Control (GPC):

$$J(N_1N_2N_3) = \sum_{j=N_1}^{N_2} \beta(j)[\hat{y}(k+j/k) - \omega(k+j)^2] + \sum_{j=1}^{N_u} \lambda(j)\,[u(k+j-1)^2] \quad (2.22)$$

Where N_1 and N_2 are the lower and upper prediction horizons over the output, N_u is the control horizon, $\beta(j)$, $\lambda(j)$ are weighting factors. The control horizon permits to decrease the number of calculated future control according to the relation: $\Delta u(K+j) = 0 \text{ for } j \geq N_u$ and $\omega(K+j)$ represents the reference trajectory over the future horizon, N. Constraints over the control signal, the outputs and the control signal changing can be added to the cost function as follows:

$$u_{min} \leq u(k) \leq u_{max}$$

$$\Delta u_{min} \leq \Delta u(k) \leq \Delta u_{max}$$

$$y_{min} \leq y_k \leq y_{max}$$

Solution of equation (2.22) gives the optimal sequence of control signal over the horizon N while respecting the given constraint. MPC have many advantages, in particularly it can pilot a big variety of process, being simple to apply in the case of multivariable system, can compensate the effect of pure delay by the prediction, inducing the anticipate effect in closed loop, sometimes being a simple technique of control to be applied and also offer optimal solution while respecting the given constraints. On the other hand, MPC requires the knowledge of model and in the presence of constraints it becomes a relatively more complex regulator than a simple conventional controller and it takes more time for on-line calculations. The advantages and disadvantages of MPC is summarized below.

2.6.1 Advantages of Model Predictive Control

MPC have many advantages, in particularly it can pilot a big variety of process and its convenient to apply in the case of multivariable system. Also it can compensate the effect of pure delay by the prediction, inducing the anticipate effect in closed loop. It is sometimes a simple technique of control to be applied and also offer optimal solution while respecting given constraints.

2.6.2 Disadvantage of MPC

The MPC requires the knowledge of model and in the presence of constraints it becomes a relatively more complex regulator. It also takes more time for on-line calculations. Its algorithms are too complex. Sometimes, the complex algorithms of MPC are not needed when dealing with simple systems. Hence, simple and reliable methods which give the same or better performance than MPC are still necessary.

2.7 References

1] P. Kundur, Power System Stability and Control. New York: McGraw-Hill, 1994.

[2] Kia Yong Lim, Youyi Wang and Rujing Zhou "Decentralized robust load-frequency control in coordination with frequency-controllable HVDC links"

[3] Ajitha priyadarsini .S, P. Melba Mary." Load Frequency Control in Co-ordination with Frequency Controlable HDVC Links Using Fuzzy Logic Controllers" International Journal of Research in Engineering and Technology eISSN: 2319-1163 | pISSN: 2321-7308

[4]Had i Saadat, Power System Analysis, New York: McGraw-Hill, 1999, pp 527-533

[5]A. Morinec, and F. Villaseca, "Continuous-Mode Automatic Generation Control of a Three-Area Power System," The 33rd North American Control Symposium, pp. 63–70,2001.

[6] Ibraheem, P. Kumar, and D. Kothari, "Recent Philosophies of Automatic Generation Control Strategies in Power Systems," IEEE Transactions on Power Systems, vol. 20, no. 1, pp. 346–357, Feb. 2005.

[7] T. Hiyama, S. Koga, and Y. Yoshimuta, "Fuzzy Logic Based Multi-Functional Load Frequency Control," IEEE Power Engineering Society 2000 Winter Meeting, vol. 2, pp. 921–926, Jan. 2000.

[8] H. Mohamed, L. Hassan, M. Moghavvemi, and S. Yang, "Load Frequency Controller Design for Iraqi National Super Grid System Using Fuzzy Logic Controller," SICE Annual Conference, pp. 227–232, Aug. 2008.

[9] D. Rerkpreedapong, A. Hasanovic, and A. Feliachi, "Robust Load Frequency Control Using Genetic Algorithms and Linear Matrix Inequalities," IEEE Transactions on Power Systems, vol. 18, no. 2, pp. 855–861, May 2003.

[10] T. H. Mohamed, H. Bevrani, A. A. Hassan, T. Hiyama. Decentralized model predictive based load frequency control in an interconnected power system. Energy Convers Manage 2011; 52:1208–41.

[11] M. Kothari, N. Sinha and M. Rafi, "Automatic Generation Control of an Interconnected Power System under Deregulated Environment," Power Quality, vol. 18, pp. 95–102, Jun. 1998.

[12] V. Donde, M. A. Pai, and I. A. Hiskens, "Simulation and Optimization in an AGC System after Deregulation," IEEE Transactions on Power Systems, vol. 16, pp. 481–489, Aug. 2001.

[13] M. Aldeen, and R. Sharma, "Robust Detection of Faults in Frequency Control Loops," IEEE Transactions on Power Systems, vol. 22, no. 1, pp. 413–422, Feb. 2007.

[14] M. Rahi, and A. Feliachi, "H∞ Robust Decentralized Controller for Nonlinear Power Systems," The 30th Southeastern Symposium of System Theory, pp. 268–270, Mar. 1998.

[15] A. Paradkar, A. Davari, and A. Feliachi, "Disturbance Accommodation Control versus Conventional Control, in LFC of a Two Area Distribution System in a Deregulated Environment," The 35th Southeastern Symposium on System Theory, pp. 98–102, Mar.2003.

[16] S. Ohba, H. Ohnishi, and S. Iwamoto, "An Advanced LFC Design Considering Parameter Uncertainties in Power Systems," Proceedings of IEEE conference on Power Symposium, pp. 630–635, Sep. 2007.

[17] [5]Araki, M. Control system, robotic and automation-Vol. I- PID control

[18] Joseph DiStefano, Allen R. Stubberud, Ivan J. Williams, Schaum outline of Theory and Problems of Feedback and Control Systems, Mcgraw-Hill,pp.112-114

Chapter 3

Coefficient Diagram Method

3.1 Introduction

This Chapter discusses the CDM, its design, problems and modification. The CDM, which was recently developed and introduced by Prof. Shunji Manabe in 1991 is referred to in this work as the standard CDM. It is an algebraic approach applied to a polynomial loop in the parameter space, where a special diagram called coefficient diagram, is used as the vehicle to carry the necessary design information, and as the criteria of good design [1].

Although, CDM is a new method, its main principles have been used in the industry over 40 years [1,2] with successful application in servo control, steel mill drive control, gas turbine control, and spacecraft attitude control.

3.2. The standard CDM

In general, the classical control and modern control are mainly used in control design; however, there is a third approach generally known as algebraic design approach [1]. The Coefficient Diagram Method (CDM) is one of the algebraic design approaches, where the coefficient diagram is used instead of Bode diagram, and the sufficient condition for stability by Lipatov constitutes its theoretical basis [3,4].

The CDM is a technique to arrange the poles of a closed loop transfer function, in order to get wanted response in the time domain [2, 5]. It provides information on the stability, time response and robustness characteristics of systems in a single diagram, which is important for systems with large characteristic polynomial degree. In a coefficient diagram, logarithmic vertical axis shows the coefficients of characteristic polynomial (a_i), stability indices (γ_i) and equivalent time constant (τ); whereas the horizontal axis shows the order i values corresponding to each coefficients. The degree of convexity obtained from coefficients of the characteristic polynomial gives a measure of stability, whereas the general inclination of the curve gives the measure of the speed of response. The shape of the a_i curve due to plant's parameter variation gives a measure of robustness.

The block diagram of a single input single output (SISO) linear time invariant (LTI) system with CDM control is shown in figure 3.1, where $N(s) = B_p(s)$ is numerator polynomial, $D(s) = A_p(s)$ is denominator polynomial of the plant transfer function, $A_c(s)$

is the forward denominator polynomial while F(s) and $B_c(s)$ are reference numerator and feedback numerator polynomials respectively.

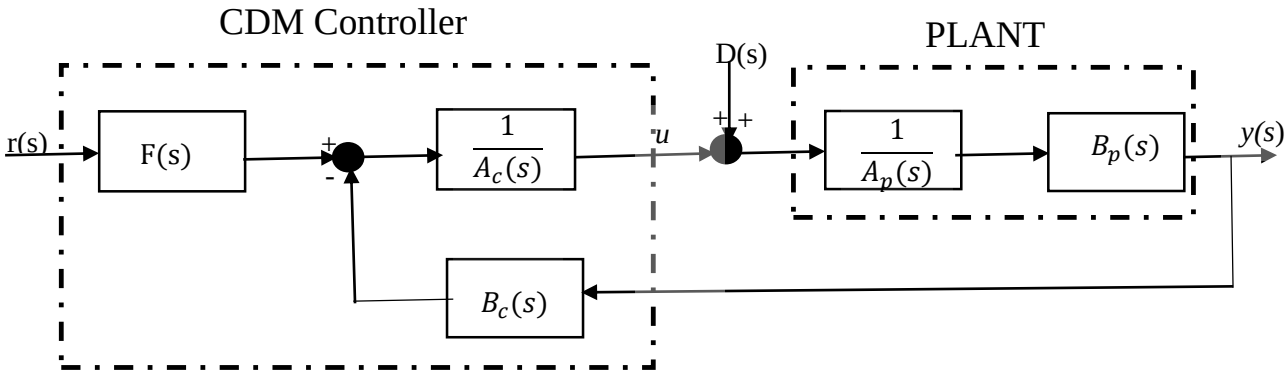

Figure 3.1. Block Diagram of a SISO LTI System with Standard CDM

Note that the subscript c stands for controller while the subscript p stands for plant respectively.

Hence, the transfer function of the controller has two numerators, which implies a 2DOF system structure. In this method *r(s)* is taken as the reference input to the system, *u* as the controller signal, and *D*(s) as the external disturbance signal. The output of the controller closed loop system, *y*, is given by

$$y = \frac{N(s)f(s)}{P(s)} \qquad (3.1)$$

where $P(s)$ is the characteristic polynomial of the closed-loop system and it is defined by

$$P(s) = A_c(s)D(s) + B_c(s)N(s) \qquad (3.2)$$

$A_c(s)$ and $B_c(s)$ are referred to as the control polynomials and defined as

$$A_c(s) = \sum_{i=0}^{p} l_i s^i \; and \; B_c(s) = \sum_{i=0}^{q} k_i s^i \qquad (3.3)$$

For practical realization, the condition $P \geq q$ must be satisfied. To get the characteristic polynomial $P(s)$, the controller polynomials $A_c(s)$ and $B_c(s)$ from (3.3) are substituted into (3.2) and this yields

$$P(s) = \sum_{i=0}^{p} l_i s^i \, D(s) + \sum_{i=0}^{q} k_i s^i \, N(s) = \sum_{i=0}^{n} a_i s^i \; , a_i > 0 \qquad (3.4)$$

CDM needs some design parameters with respect to the characteristic polynomial coefficients which are the equivalent time constant (τ) (which gives the speed of closed loop response), the stability indices (γ_i) (which give the stability and the shape of the time response), and the stability limits (γ^*). The relations between these parameters and the coefficients of the characteristic polynomial (a_i) can be described as follows:

$$\gamma_i = \frac{{a_i}^2}{a_i + i a_{i-1}}, \quad i \in [1, n-1], \gamma_0 = \gamma_i = \infty \tag{3.5}$$

$$\tau = \frac{a_1}{a_0} = \frac{t_s}{2.5} - \frac{t_s}{3} \tag{3.6}$$

$$\gamma_i{}^* = \frac{1}{\gamma_{i-1}} + \frac{1}{\gamma_{i+1}}, \qquad i \in [1, n-1] \tag{3.7}$$

According to Manabe's standard form, γ_i values are selected as $\{2.5, 2, 2 \ldots 2\}$. The above γ_i values can be changed by the designer as per the controller's requirement. However, the disadvantage is that changing the values requires experience or trial and error. Using the key parameters (τ) and (γ_i) the target characteristic polynomial, $P_{target}(s)$ can be written as:

$$P_{target}(s) = a_0 \left[\left\{ \sum_{i=2}^{n} \left(\Pi_{j=1}^{i-1} \frac{1}{\gamma^j{}_{i-j}} \right) (\tau s)^i \right\} + (\tau s) + 1 \right] \tag{3.8}$$

where $P(s) = P_{target}(s)$.

Also, the reference numerator polynomials $F(s)$ can be callculated from:

$$F(s) = \left(\frac{P(s)}{N(s)} \right) \Bigg|_{s=0} \tag{3.9}$$

3.2.1 Challenge(s) involving the Use of Standard CDM in Power system Control

Even though the standard CDM is simple and has been proven to be robust, several challenges may be involve when implementing it into power system as a standalone controller especially for LFC. One of the important challenges has to do with the fact that due to the complexity of power system structure and the constant changes occurring within a power system, tuning of the CDM parameters for power system frequency control becomes a problem. For example, the standard values of the stability indices of the standard CDM, when utilized, will not give desirable performance due to power system complexity and constant changes. Therefore, these

parameters of the standard CDM such as stability indices have to be changed and new values of stability indices must be chosen. However, choosing new values of the stability indices is done based on experience of the designer or by trial and error approach. This is a serious problem especially for new power system control designers. The next chapter discusses a solution to the problem by modifying the standard CDM.

3.3. The Proposed CDM

This section discusses a design method of the proposed CDM to meet desired performance criteria. The parameters of proposed controller are designed based on the stability and the speed of the Controlled system.

Stability is designed from the standard stability index, γ_i, and speed is designed from the equivalent time constant, τ, and the tuning factor α. The stability index, the equivalent time constant, and the tuning factor are defined based on the closed-loop transfer function. These coefficients are related to the controller parameters algebraically in an explicit form.

A feed forward and feedback compensators are introduced and added to the standard CDM so as to effectively employ the parameters of controller as shown in figure 3.2. The compensators can also cause an exchange in signals from outside of the feedback-loops which can ensure the overall stability of the power system.

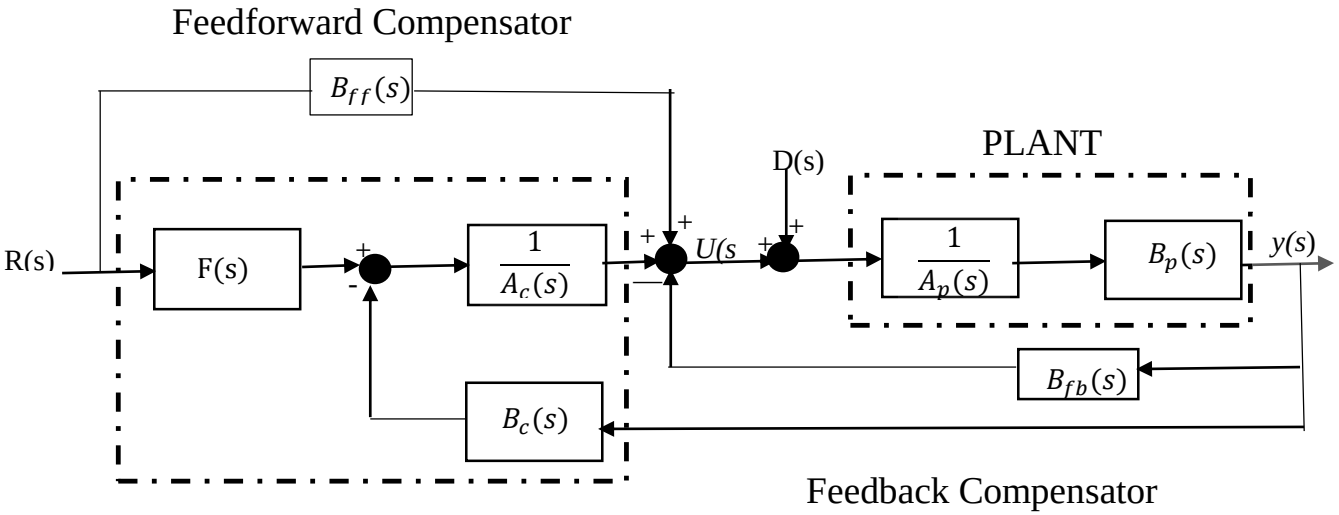

Figure 3.2. Implementation of the Proposed CDM

In the figure,$B_{ff}(s)$ and $B_{fb}(s)$ are the polynomials of the feed forward compensator

and the feedback compensator respectively. After rearranging the plant and the feedback compensator shown in $A^*_p(s)$ and $B^*_p(s)$ which are the polynomials of the modified plant can be obtained and as shown in figure 3.3 below. From the block diagram of the modified plant in figure 3.3,

$$\frac{y(s)}{R(s)} = \frac{B^*_p(s)[F(s) + B_{ff}(s)A_c(s)]}{A_c(s)B^*_p(s) + B_c(s)B^*_p(s)} \dots\dots\dots\dots\dots\dots\dots\dots (3.10)$$

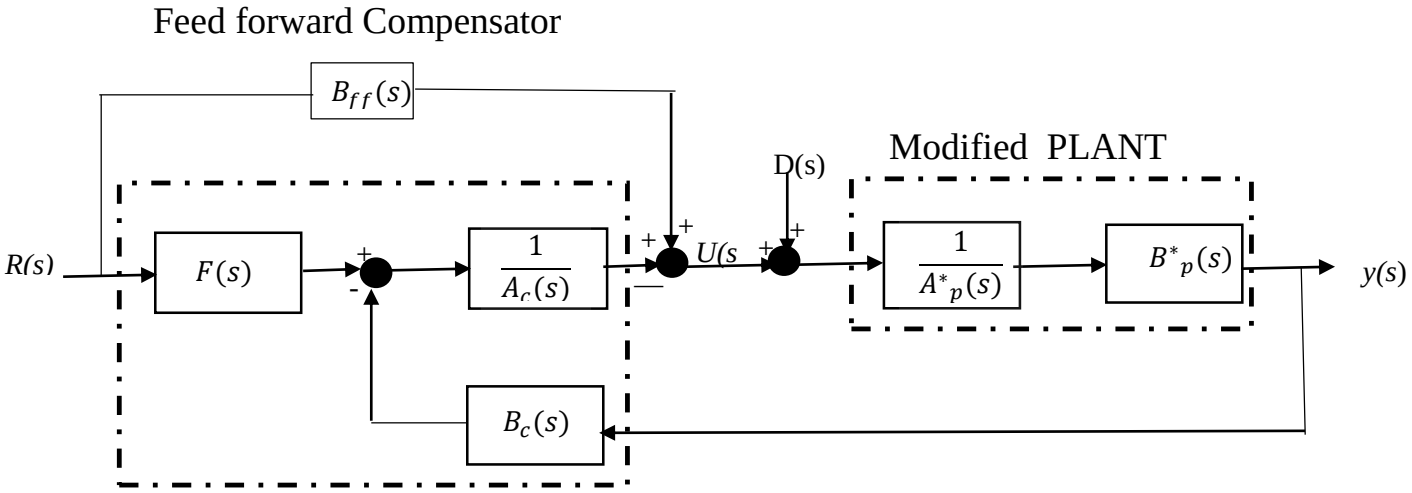

Figure 3.3. Proposed CDM after modification

while

$$\frac{y(s)}{D(s)} = \frac{A_c(s)B^*_p(s)}{A_c(s)A^*_p(s) + B_c(s)B^*_p(s)} \dots\dots\dots\dots\dots\dots\dots\dots (3.11)$$

Equation (3.10) shows that the feed forward compensator $B_{ff}(s)$ affects the transfer function from the system input *R(s)* to the output *y(s)* and can be used to increase the speed of the transient response of the controlled system. On the other hand equation (3.11) shows that the transfer function from *D(s)* to *y(s)* is not affected. Hence, the feed forward compensator has an influence on the system from the reference input to the output and can be used to increase the speed of the transient response without affecting the transfer function from the disturbances to the output

Finally, in order to design the propose controller in term of γ_i, τ and α, equation (3.10) is assumed as

$$\frac{y(s)}{R(s)} = \frac{A(s)}{B(s)} = \frac{b_m s^m + b_{m-1}s^{m-1} + \cdots + b_1 s + b_0}{a_n s^n + a_{n-1}s^{n-1} + \cdots + a_1 s + a_0} \quad (3.12)$$

Where $m \leq n$ and the value of all a's and b's are constant. The denominator polynomial $A(s)$ is the characteristic polynomial of the proposed control system, and

its coefficients can be found from

$$A(s) = a_0 \left[\left\{ \sum_{i=2}^{n} \left(\Pi_{j=1}^{i-1} \frac{1}{\gamma^j{}_{i-j}} \right) (\tau s)^i \right\} + (\tau s) + 1 \right] \quad (3.13)$$

Note that equation (3.13) is the same form as equation (3.8), the equation for the target polynomials. The CDM is mainly used to design the controller of the closed-loop system. However, this method can also be extended to design the coefficients of the numerator polynomial B(s) as well [6-7]. Thus, the relationship among the coefficients of the numerator polynomial B(s) can be defined as

$$b_i = (b_0 \alpha \tau)^i \frac{1}{\gamma_{i-1} \cdots \gamma^{i-2} \gamma^{i-1}} = (b_0 \alpha \tau)^i \prod\nolimits_{j=1}^{i-1} \frac{1}{\left(\gamma_{i-j}\right)^j} \ldots\ldots (3.14)$$

where α is the tuning factor. The equivalent time constant τ is scaled by tuning factor α so that the response speed can be adjusted. The value of tuning factor α is defined as $0 \leq \alpha \leq 1$. Substituting each coefficient b_i into the numerator polynomial B(s) leads to

$$B(s) = b_0 \left[\left\{ \sum_{i=2}^{m} \left(\prod\nolimits_{j=1}^{i-1} \frac{1}{\gamma^j{}_{i-j}} \right) (\alpha \tau s)^i \right\} + (\alpha \tau s) + 1 \right] \quad (3.15)$$

Hence the proposed controller in terms of γ_i, τ and α can be obtained by

$$\frac{y(s)}{R(s)} = \frac{b_0 \left[\left\{ \sum_{i=2}^{m} \left(\prod_{j=1}^{i-1} \frac{1}{\gamma^j{}_{i-j}} \right) (\alpha \tau s)^i \right\} + (\alpha \tau s) + 1 \right]}{a_0 \left[\left\{ \sum_{i=2}^{n} \left(\Pi_{j=1}^{i-1} \frac{1}{\gamma^j{}_{i-j}} \right) (\tau s)^i \right\} + (\tau s) + 1 \right]} \ldots\ldots (3.16)$$

This transfer function is a general form for designing the proposed CDM control system. The parameters can be designed by:

- Derive the transfer function (15) which contains the unknown parameters of proposed controller. In this step, a designer must select the number of the feedforward and the feedback parameters. Usually, the number of feedback parameters should equal to the order of the plant.
- Define the settling time t_s in order to find the equivalent time constant τ from equation (3.6). Then determine the proper values of stability indices and tuning factor. After that, substitute these parameters to equation (3.16). Note that t_s cannot be specified in case that the number of the feedback compensator parameters is less than the order of the plant.
- Finally, the parameters of the propose controller are obtained simultaneously by equating the (3.10) and (3.16)

3.3.1 Proving the Need for the Propose Scheme by Simulation

Mathematical explanations above show that the compensators will enhance the frequency stability of the power system by compensating for deficient performances. However, these mathematical expressions are of no technological significance if they cannot be experimentally proven. One way to prove that the standard CDM would not work for power system using the standard stability indices is by computer simulation. A mathematical model of a power system is developed. Then a sudden load change occurred on the power system and the frequency deviation step response obtained.

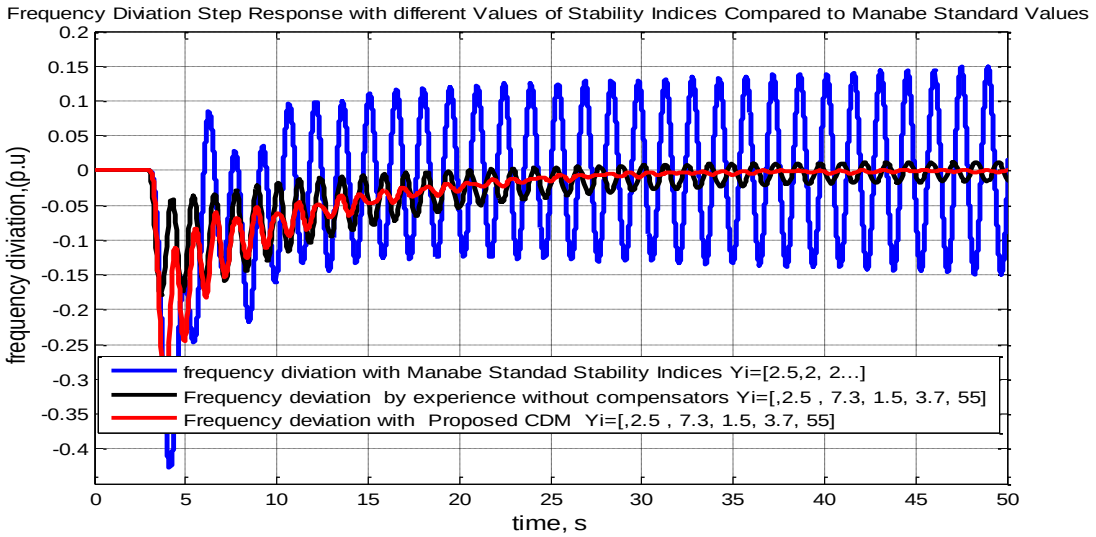

Figure 3.4. Frequency deviation step response: deficient performance compensated by proposed CDM

Figure 3.4 above shows the frequency deviation step response of the single area power system. Since the same power system is utilized in Chapter 5, the parameters of the power system can be found there. Unlike chapter 5 where more complicated cases such as integration of windfarm is consider, this simulation only considers sudden change in load.

It can be seen that the value of the stability index has effect on the disturbance rejection capability. With the standard Manabe values used, the system goes out of step. When the stability indices where changed based on experience, it can be observed that there is no overshoot, and steady-state error is reduced. Also, it is clear that the value obtained based on experience still needs to be changed to get better result since it takes much longer time before the power system can get stable. Finally, it can also be seen that when the proposed CDM is implemented, the deficient

performance is compensate. Hence the frequency deviation is zero and the frequency returns to nominal value.

Having seen that the Manabe standard CDM has a disadvantage when implemented into power system for frequency control; and having seen that the proposed control scheme will compensate the deficient performance of the standard CDM controller, then the question is, is the proposed controller suitable for power system frequency control considering various power system configurations? Digital simulation can help find answer to this question and this is done in the next chapter where the proposed CDM is compared to MPC and conventional integral control considering various power system configurations.

3.4 References

[1] S. Manabe, "Coefficient Diagram Method", 14th IFAC Symp on Automatic Control in Aerospace, Seoul, 1998.

[2] Shunji Manabe, “Importance of Coefficient Diagram in Polynomial Method”, Proceedings of the 42nd IEEE Conference on Decision and Control Maui, Hawaii USA, December 2003

[3]. A. Lipatov and N. Sokolov, Some sufficient conditions for stability and instability of continuous linear stationary systems , Automat. Remote Cont., 39, 1285-1291, 1979.

[4]. S. Manabe, Sufficient condition for stability and instability by Lipatov and its application to the CDM , 9th Workshop on Astrodynamics and Flight Mechanics, Sagamira, ISAS, 1999

[5] Rinu raj RR, Vijay LD, Anand C. Design and implementation of a CDM-PI controller for a spherical tank level system. Int J Theor Appl Res Mech Eng (IJTARME) 2013;2(1).

[6] D.Isarakorn, S.Panaudomsup, T.Benjanarasuth, J.Ngamwiwit, and N.Komine. “Application of CDM to PDFF Controller for Motion Control System,” The 4th Asian Control Conference, 2002, pp. 1173-1177.

[7] D.Kumpanya, T.Benjanarasuth, J.Ngamwiwit, and N.Komine. “PI Controller Design with Feedforward by CDM for Level Process,” TENCON2000, Vol. 2, 2000, pp. 65-69.

Chapter 4

First Case Study: Application of CDM to Interconnected Power System for Decentralized Frequency Control

4.1 Introduction

Since Liberia, Guinea and Sierra Leone have the lowest electric power access rate in the world [1], it is necessary to study their interconnection for stability enhancement of developing countries' power systems. Therefore, in this work it is assumed that each country represents one control area; and with that, a two and three area power systems similar to their interconnections are modelled. First, a two area power system is modelled and analyzed as a test system. This test system is assumed similar to the interconnection of Liberia and Sierra Leone. After modeling and analysis of the two area power system, then the three area power system assumed similar to the interconnection of Liberia, Guinea and Sierra Leone is also modelled for frequency enhancement studies. The proposed CDM is then implemented as control strategy to promote reliable power distributions.

To validate the effectiveness of the proposed CDM, digital simulations of are carried out comparing the proposed CDM to the PI-controller and MPC. Details of the simulations and discussions are found in this chapter.

4.2 The Assumed Interconnected Power System

In November 2013 the African Development Bank (AFDB) approved the Côte D'Ivoire, Liberia, Sierra Leone and Guinea (CLSG) electricity networks interconnection project which will secure power supply for the Mano River Union (MRU) member countries, and will be implemented between 2014 and 2017 [1].

The CLSG project involves the construction of high voltage lines to interconnect the four countries where at least three regional control centers are expected.

4.2.1 The Mano River Union (MRU)

The MRU is an international association established in 1973 between Liberia and Sierra Leone. In 1980, Guinea joined the union. The goal of the Union was to foster economic cooperation among the countries. It is named after the Mano River, a river

which begins in the Guinea highlands and forms a border between Liberia and Sierra Leone.

Due to internal conflicts among the countries, the objectives of the Union could not be achieved. However, on May 20, 2004, the Union was reactivated at a summit of the three leaders of the Mano River Union states and on April 1, 2008, Cote D'Ivoire agreed to join the union.

Figure 4.1 shows the map of Africa in which member states of the MRU are shown in blue

Figure 4.1. Member states of MRU

4.3. Need of Interconnection within the Mano River Union [2]

The electricity sector in the Mano River Union countries faces major constraints such as:

- low access to electricity;
- a structural deficit in the supply of electricity;
- a preponderance of thermal generation in the energy mix;
- low financial and institutional capacities of national electricity companies.

Therefore, the CLSG project is intended to increase the average rate of access to electricity in the four countries from 28 per cent to 33 per cent, electrifying 125 locations along the transmission line as well as 70 schools, 30 health centers and nearly 1,500 small commercial and industrial craft enterprises, of which 25 per cent are held by women. It is expected that 24 million inhabitants who are affected will enjoy reliable electric power at a competitive cost.

The interconnection of the MRU power systems will form the backbone of the Mano River Union countries and is one of the priority projects of the West African Power Pool (WAPP) Master Plan, a cooperation initiative linking national electricity companies in West Africa. Thus, the CLSG project will contribute to the future of power system interconnections in West Africa. It also involves various planning and feasibility studies on hydropower plants that could enhance energy exchange. Since the MRU countries are emerging from long sociopolitical crises and have problems of

low levels of investment in in recent years, power infrastructure operate below standard, and their services are extremely poor. The cost of electric power production per kWh remains very high in those countries where the electricity access rate is among the lowest in the world (two per cent in Liberia and Sierra Leone; 10 per cent in Guinea).

Therefore, the construction of the interconnected power system will foster the development of the huge hydroelectric potential of the sub-region by offering the possibility of electric power trade between the countries within the larger West African market, thus contributing to regional integration.

4.4 The proposed CDM Application to Two Area Interconnected Power System

First, a two-control area power system assumed similar to the interconnection of Liberia and Sierra Leone shown in figure 4.2 is considered as a test system to illustrate the effectiveness of the proposed control strategy. Each area consists of the overall rotating mass and load, and an aggregated generator unit including one nonlinear turbine with generation rate constraint GRC, and one governor with dead-band constraint [3].

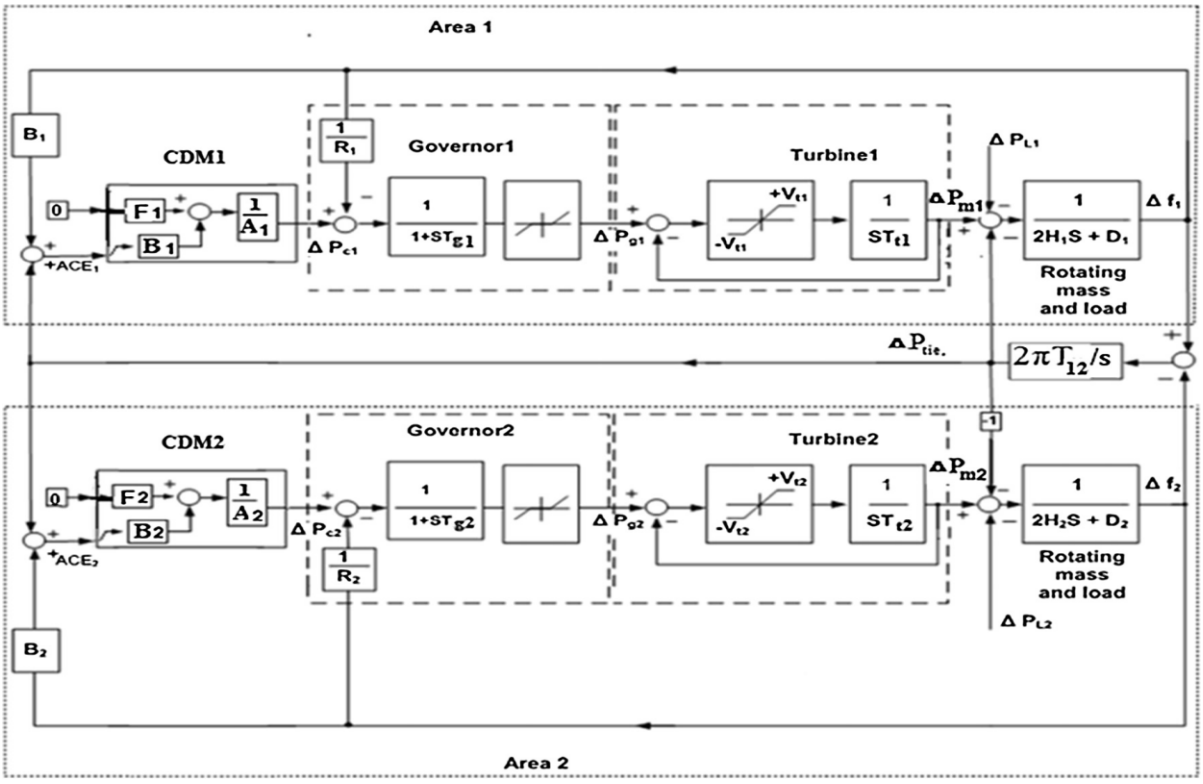

Figure 4.2. The block diagram of two area power system including the proposed CDM controllers

As a decentralized control system, each local area controller has been designed independently. On the other hand, the frequency deviation is used as a feedback for the closed loop control system. The measured and reference area control error, ACE_i, ($ACE_{ref} = 0\ Hz$) are fed to the proposed CDM controller in order to obtain the supplementary control action ΔP_{ci} which adds to the negative frequency feedback signal. The resulting signal is fed the governor giving the governor valve position which supplies the turbine to give the mechanical power change ΔP_{mi}. This mechanical power change (ΔP_{mi}) is then affected by the load change ΔP_{Li} and the tie-line power change, ΔP_{tiei} . This effect gives input of the rotating mass and load block to provide the actual frequency deviation, Δf . In addition, the tie-line flow deviation is added to the frequency deviation in the supplementary feedback loop to give the area control error, ACE_i.

4.4.1 Results and Discussion

Computer simulations have been carried out for validating the effectiveness of the proposed scheme. Matlab/Simulink software package has been utilized for this purpose. Since the power system interconnecting MRU countries has only been approved and yet to be completed, this work therefore utilized parameters from reference [3], thus considering the following nominal parameters listed in table 4.1 below.

Table 4.1 Parameters and data of the two area power system.

Area	K(s)	$\boldsymbol{D}$(**pu /Hz**)	2H(pu.sec)	R(Hz/pu)	T_g(sec)	T_t(sec)	T_{12}
Area 1	-0.3/s	0.015	0.1667	3.00	0.08	0.40	0.20
Area 2	-0.2/s	0.016	0.2017	2.73	0.06	0.44	

The proposed CDM is designed based on the stability indices *($\gamma_{i,1}$)* utilized and the parameters are set as follows:

The time constant $\tau = 2$ sec., k_0=40,
$D_1 = 0.348S + 0.1739S^2 + 0.0805S^3 + 0.005334S^4$
$N_1 = 1.256 + 0.3483S$
the stability indices ($\gamma_{i,1}$) have been selected as:
$\gamma_{i,1} = [1, 6.5, 1.5, 2.7, 72]$ $, i \in [1,5]$ $, \gamma_0 = \gamma_6 = \infty$
And the stability limits($\gamma_{i,1}$*) are:
$\gamma^*_{i,1} = [0.153, 1.66, 0.523, 0.68, 0.0138]$ $, i \in [1,5]$
$P_{tareget,1} = 50 + 100S + 202.18S^2 + 61.161S^3 + 12.42S^4 + 0.96S^5 + 0.001S^6$
$B_1 = 40 + 69S + 100S^2$
$A_1 = 150S + 2S^2$
Tuning factor $\alpha = 0.75$

$D_2 = 0.382S + 0.2097S^2 + 0.10127S^3 + 0.00532S^4$
$N_2 = 1.256 + 0.3827S$
the stability indices ($\gamma_{i,2}$) have been selected as:
$\gamma_{i,2} = [1, 6.4, 2.3, 1.53, 3.5]$ $, i \in [1,5]$ $, \gamma_0 = \gamma_6 = \infty$
And the stability limits($\gamma^*_{i,2}$) are:
$\gamma^*_{i,2} = [0.1562, 1.434, 0.809, 0.7179, 0.653]$ $, i \in [1,5]$
$P_{tareget,2} = 40 + 80S + 160.7S^2 + 51S^3 + 6.6S^4 + 0.6S^5 + 0.015S^6$
And choosing k_0=32, then
$B_2 = 32 + 54S + 100S^2$
$A_2 = 60S + 3S^2$
Tuning factor $\alpha = 0.58$

The simulation studies are carried out for the proposed controllers with generation rate constraint (GRC) of 10% per minute and the maximum value of dead band for governor is specified as 0.05 pu for each area [2].

4.4.1.1 Case i: Norminal Case, proposed CDM vs Conventional PI Controller

The system performance with the proposed CDM controllers at nominal parameters is tested and compared with the system performance with a conventional PI controller and at only load change in area-2. Figure 4.3 below shows the simulation results in this case.

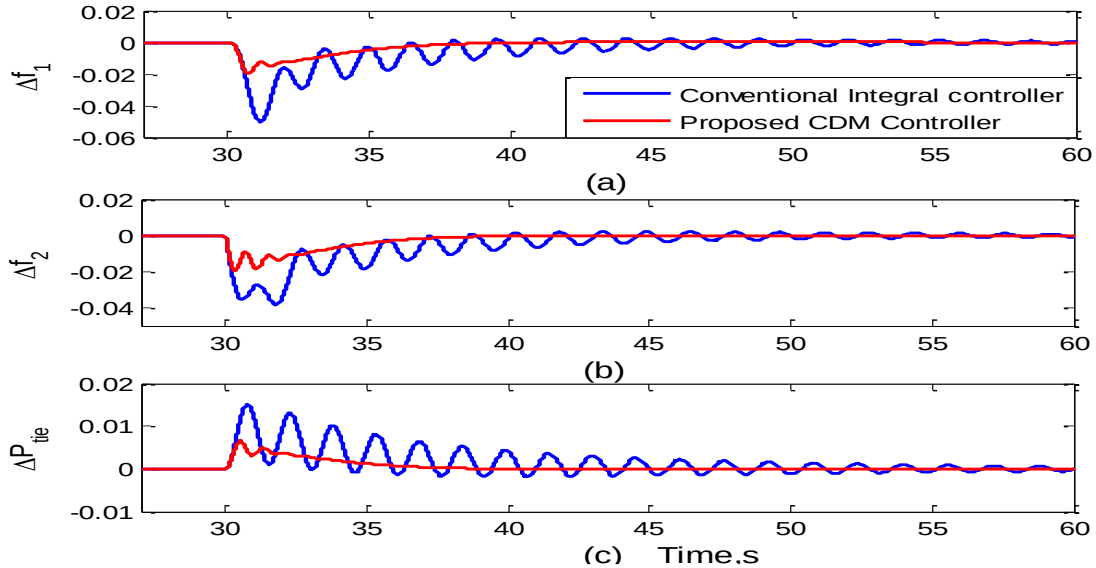

Figure 4.3. Power system responses to case 1 (a) frequency deviation in area-1, (b) frequency deviation in area 2 and (c) tie-line power change.

The results from the top to the bottom are: the frequency deviations of area-1 Δf_1, the frequency deviations of area-2 Δf_2, and the tie-line power change between area-and area-2 using both the proposed CDM and classical PI controllers following a step load change in area-2 (ΔP_{L2} assumed to be 0.02 pu at time, *t = 30s*.). It is observed

that with the proposed CDM controller the system is more stable and fast comparing with the system with traditional PI. This is because the tuning factor contributed by the feed forward compensator affects the response speed significantly.

4.4.1.2 Case ii: Robustness Evaluation, Propose CDM vs Conventional PI Control

The robustness of the proposed CDM controller against wide range of parameter uncertainty is validated. In this case, the governor and turbine time constants of the two areas are increased to T_{g1} = *0.105s* (≅31% change), T_{t1} = *0.785s* (≅95% change), T_{g2} = *0.105s* (≅66% change) and T_{t2}= *0.6s* (≅ 38% change), respectively. Figure 4.4 below depicts the response of the CDM controllers in the presence of above uncertainty, at same load change described in the first case.

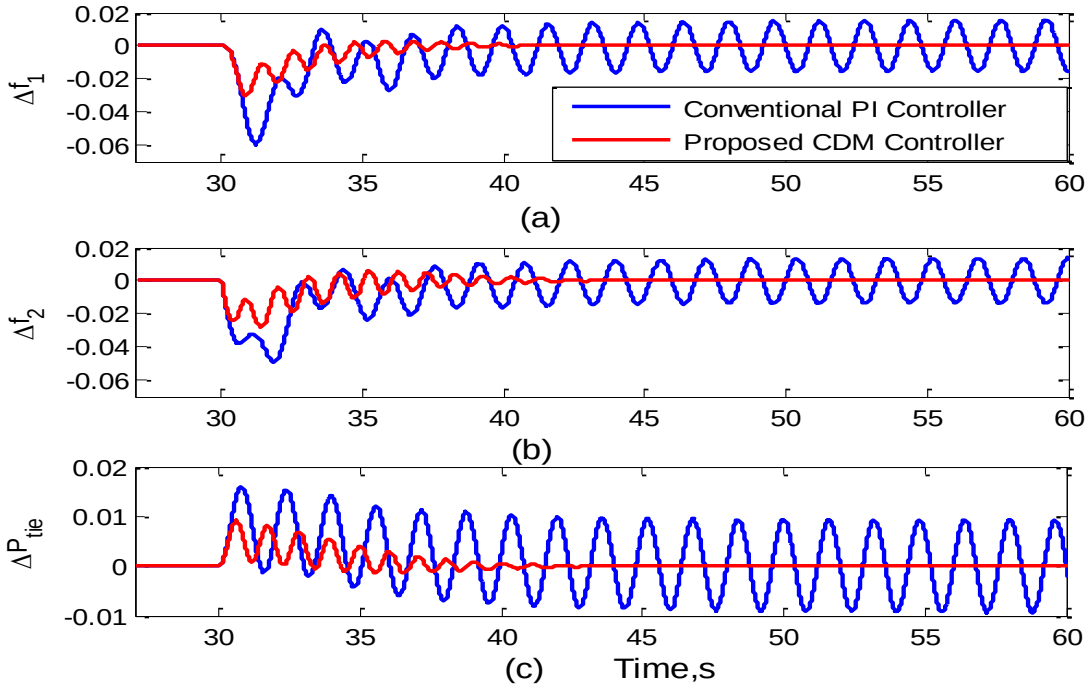

Figure 4.4. Power system responses to case 2 (a) frequency deviation in area-1, (b) frequency deviation in area 2 and (c) tie-line power change.

It has been indicated that a desirable performance response has been achieved using the CDM controller while with conventional PI, the performance and stability are seriously degraded.

4.5 Application on the Assumed Three Area Interconnected Power System

Assume a three area interconnected power system as shown in figure 4.5 similar to the interconnection of Liberia, Guinea and Sierra Leone.

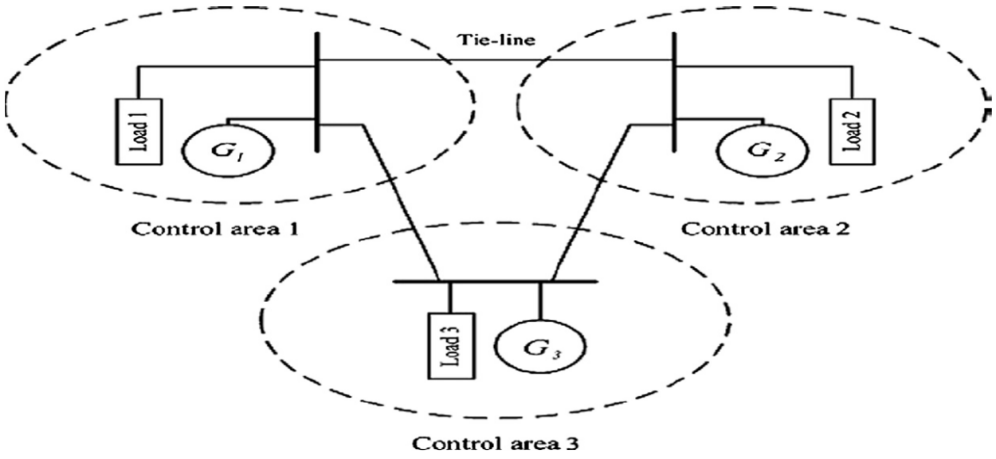

Figure 4.5. Three-control area power system.

It has previously been stated that these MRU countries have mainly been considered for assumption in this work because their power systems have not only the worst power quality in the world. Also these countries have the lowest electricity access rate. Hence, it is necessary to model a power system similar to their interconnection, and design a frequency controller to enhance the power quality.

Since the proposed CDM is being used as a robust frequency controller, its robustness is thus tested on the three area interconnected power system in figure 4.5. It is seen in section 4.4.1.2 that in both nominal case and robust performance scenarios, the proposed CDM is far better than conventional PI controller. Therefore, this section will evaluate the CDM for further robust performance by comparing it to MPC [3], but only for the assumed three-area interconnected power system. The simulation parameters [2] are given in Table 4.2 below.

Table 4.2 Parameters and data of the three control area power system.

Area	K(s)	D(pu /Hz)	$2H$(pu.sec)	R(Hz/pu)	T_g(sec)	T_t(sec)	T_{ij}
Area-1	-0.3/s	0.015	0.1667	3.00	0.08	0.40	T_{12}=0.20
							T_{13}=0.25
Area-2	-0.2/s	0.016	0.2017	2.73	0.06	0.44	T_{21}=0.20
							T_{23}=0.15
Area-3	-0.4/s	0.015	0.1247	2.82	0.07	0.3	T_{31}=0.25
							T_{32}=0.15

$(P_e)_{Base}$=800MVA

The system is tested at a simultaneous load step disturbances of 0.02-pu in control area-2 at *t=3.0s*. It is also tested and validated against wide range of parameter uncertainties. In the tested scenarios, the governor and turbine time constants of the two areas are increased to T_{g1} = *0.105s* (≅31% change), T_{t1} = *0.785s* (≅95% change), T_{g2} = *0.105s* (≅66% change) and T_{t2}= *0.6s* (≅ 38% change), $T_{g3} = 0.15\ s$ (≅100% change) and $T_{t3} = 0.7s$ (≅100% change) respectively.
The parameters of the CDM controller of each area are set as follows:
The time constant can be taken as $\tau = 1\ s$. for all three controllers and choosing $k_{0,1}$=23, $k_{0,2}$=31 and $k_{0,3}$=30, then
$D_1 = 0.348S + 0.1739S^2 + 0.0805S^3 + 0.005334S^4$
$N_1 = 2.826 + 0.3483S$
the stability indices ($\gamma_{i,1}$) have been selected as:
$\gamma_{i,1} = [0.24, 18.28, 0.76, 3.96, 8.66] \quad , i \in [1,5] \quad , \gamma_0 = \gamma_6 = \infty$
and the stability limits($\gamma^*_{i,1}$) are:
$\gamma^*_{i,1} = [0.054, 5.475, 0.306, 1.42, 0.2525] \quad , i \in [1,5]$
$P_{tareget,1} = 65 + 65S + 263.32S^2 + 61.7S^3 + 18.5S^4 + 1.4S^5 + 0.001S^6$
$B_1 = 23 + 20.16S + 63S^2$
$A_1 = 225S + 2S^2$
And the tuning factor is $\alpha = 0.65$

D_2= $0.382S + 0.2097S^2 + 0.10127S^3 + 0.00532S^4$
N_2=$2.009 + 0.3827S$
With the stability indices ($\gamma_{i,2}$)have been selected as:
$\gamma_{i,2} = [0.179, 16.97, 1.66, 3.3, 5.26] \quad , i \in [1,5] \quad , \gamma_0 = \gamma_6 = \infty$
the stability limits($\gamma^*_{i,2}$) are:
$\gamma^*_{i,2} = [0.0589, 6.188, 0.3619, 0.7925, 0.303] \quad , i \in [1,5]$
$P_{tareget,2} = 64 + 64S + 357.5S^2 + 117.68S^3 + 23.28S^4 + 1.4S^5 + 0.016S^6$
$B_2 = 31 + 24S + 131S^2$
$A_1 = 225S + 2S^2$
And the tuning factor is $\alpha = 0.68$

D_3= $0.3696S + 0.1302S^2 + 0.0464S^3 + 0.00262S^4$
N_3=$2.3236 + 0.3692S$
And with stability indices ($\gamma_{i,3}$) have been selected as:
$\gamma_{i,3} = [0.156, 33.17, 1.56, 2.28, 6.31] \quad , i \in [1,5] \quad , \gamma_0 = \gamma_6 = \infty$
the stability limits($\gamma^*_{i,3}$) are:
$\gamma^*_{i,3} = [0.0301, 7.051, 0.4681, 0.799, 0.438] \quad , i \in [1,5]$
$P_{tareget,3} = 69.7 + 69.7S + 446.739S^2 + 86.328S^3 + 10.07S^4 + 0.58S^5 + 0.005S^6$
$B_3 = 30 + 25S + 152.5S^2$
$A_3 = 225S + 2S^2$
And the tuning factor is $\alpha = 0.73$

As seen, figure 4.6 below shows the response of the proposed CDM, MPC and conventional PI controllers in the presence of above uncertainties.

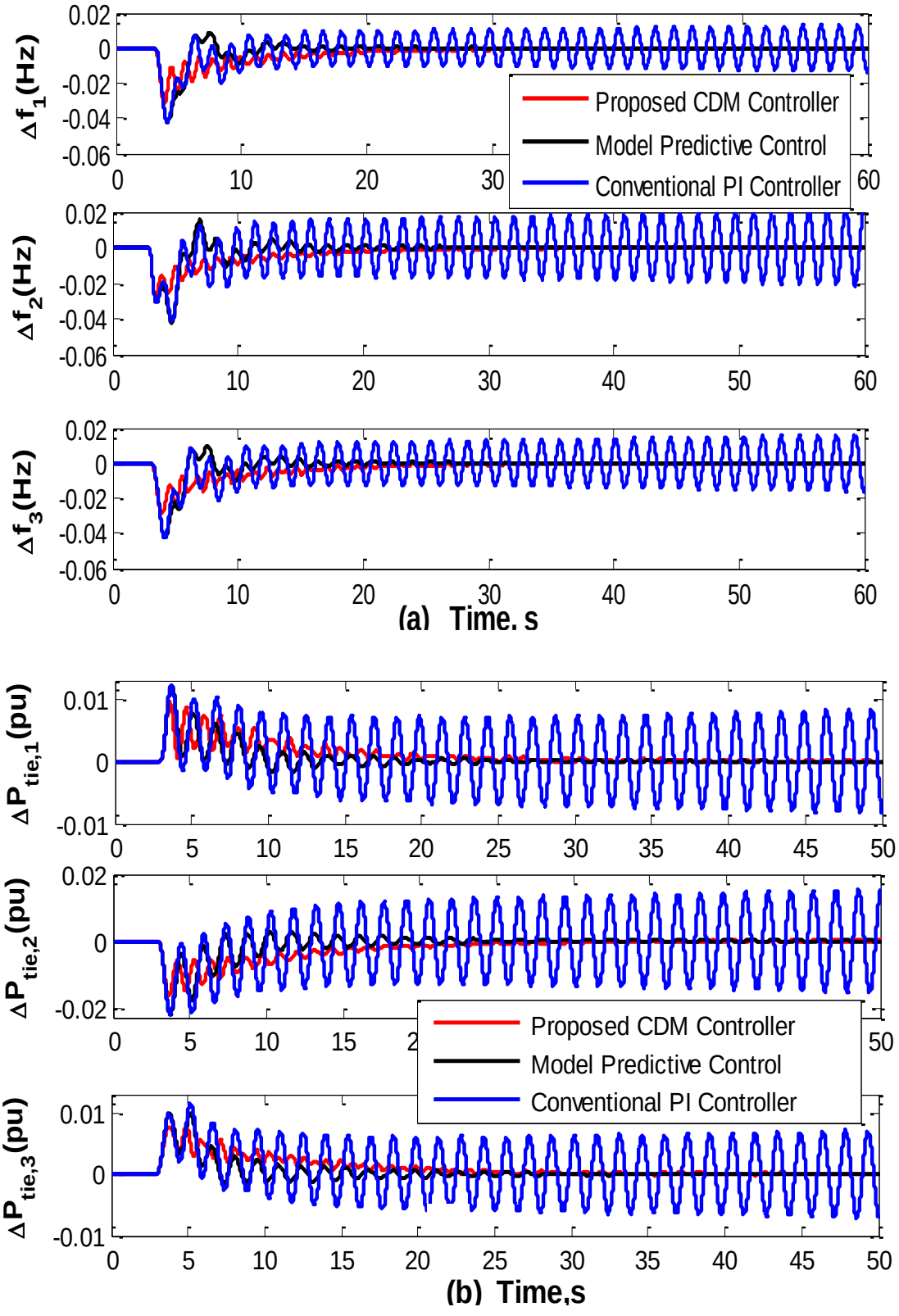

Figure 4.6. System response to case 3: (a) frequency deviations and (b) tie-line powers CDM

It is shown in the figure that when the system with the conventional controller became unstable, the system with both CDM and MPC controllers still give robust response verses load change and parameters uncertainties. In addition, even though the difference in the result for the CDM and MPC seem negligible, the tie-line powers and the frequency responses of the system with the proposed CDM show slightly better performance than that with the MPC.

4.6 Summary

In this chapter, a robust decentralized LFC design using the proposed CDM has been is investigated for an interconnected power system. The proposed method was applied to both two and three-control area power systems assumed similar to the interconnections power system of three MRU countries, namely Liberia, Sierra Leone and Guinea; and was tested, considering different load changes and parameters change cases. The results were compared with the results of conventional PI and model predictive controllers. Simulation results demonstrated the effectiveness of the proposed CDM methodology. It was shown that the power system with the proposed CDM controller is robust against the load change and parameter perturbation; and the system and has a more desirable performance as compared to classical PI control design, in all of the performed tested cases. Also, the simulation results indicated that both CDM and MPC controllers can give robust response verses load change and parameters uncertainties, but the proposed CDM is more practical in term of the calculation burdens which is available in the case of MPC.

4.7 References

[1] African Development Bank Group, “ Project Appraisal Report” Côte d’Ivoire, Liberia, Sierra Leone, Guinea (CLSG) Network Interconnection, October 2013

[2] African Development Bank Group, “ Liberia Country Strategy Paper 2013-2017”, ORWB Department, June 2013.

[3] H. Bevrani, "Robust Power system control", Springer, New York, 2009.

[4] T. H. Mohamed, H. Bevrani, A. A. Hassan, T. Hiyama. Decentralized model predictive based load frequency control in an interconnected power system. Energy Convers Manage 2011; 52:1208–41.

Chapter 5

Wind farm Integration to Power System

5.1 Introduction

This chapter provides a basic introduction to the relevant issues related to the integration of Wind Energy Conversion System (WECS) into power systems. Since gusts of wind do not hit all the wind turbines at the same time. Under certain conditions, the percentage variation of power output will drop with respect to the number of wind generators. This phenomenon is the result of frequency quality problems which finally affects the power quality. Hence, to achieve a significant smoothing effect, the number of wind turbines within a wind farm does not need to be very large. On the other hand, with the constant integration of WECS into power systems a number of problems still need to be investigated. This is because integration of wind farm will create new problems in relation to stability analysis, reactive power compensation, and power quality as well as voltage control assessments [1]. However, this chapter is concern with a general discussion of problems pertaining to wind farm integrations and the effect on voltage and frequency. Nevertheless, in the next chapter, frequency control which is the key objective of this research will be the primary focus.

5.2 Basic Integration Issues Related to Wind Power

The challenge that the integration of wind power poses can be illustrated using figure 5.1. In this power system, there are industries and households that consume power P_D and a wind power station that delivers power, P_w. The additional power, P_G, is produced at another location. The impedances $Z_1 - Z_3$ represent the impedances in the transmission lines and transformers between the different components. In an electric power system, such as the one illustrated in Figure 5.1, power cannot disappear. This means that there will always be a balance in this system because

$$P_G = P_D + P_L - P_w \qquad (5.1)$$

where

P_G = additional required power production;

P_D.=power consumption;

P_L= electrical losses in the impedances$Z_1 - Z_3$;

P_w= wind power production.

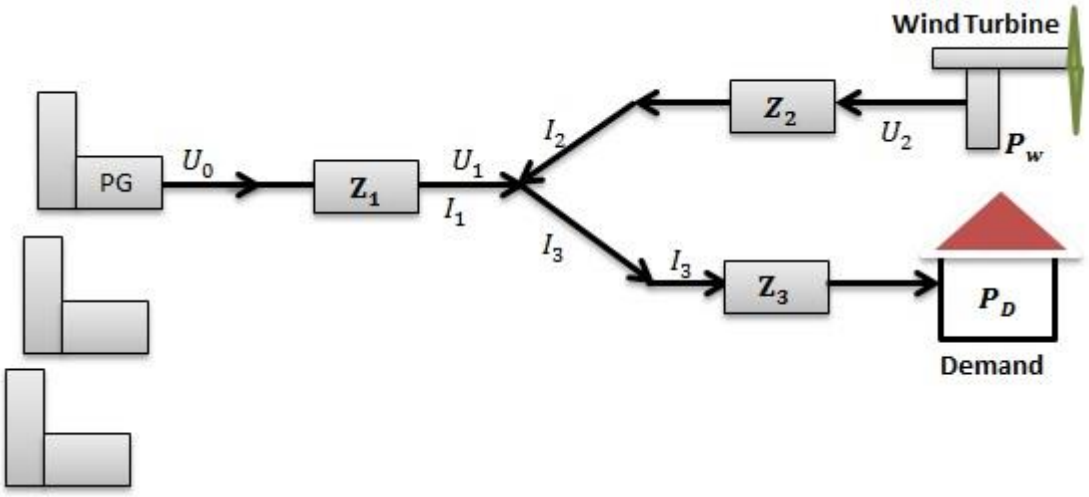

Figure 5.1. Illustrative power system

According to [2], equation (5.1) is valid for any situation; it does not matter whether we look at a short time period (e.g. minutes) or a long period (e.g. a year). It also implies that any change in electricity demand (or wind power) must be simultaneously balanced by other generation sources within the power system. For better understandings integration issues, several some requirements are discussed below.

5.2.1 Consumer requirements

As already mentioned, the main aim of a power system is to supply consumers with the required electricity at any given time at a reasonable cost. From the consumer's perspective, three main requirements can be defined as follows:

- Customer requirement 1 (CR1): The frequency of the power system and the voltage level at the connection point has to stay within an acceptable, as most customer appliances (e.g. lighting equipment, motors, computers, etc.) require a specific voltage and power range for reliable operation.
- Customer requirement 2 (CR2): the power should be available at exactly the time the consumers need it in order to use their various appliances (i.e. when a customer switches on a certain device).
- .Customer requirement 3 (CR3): the consumed power should be available at a reasonable cost (this may also include low external costs to reflect the low

environmental impact of electricity production). CR1 and CR2 also concern the reliability of the power supply. Greater reliability leads to higher costs and hence a conflict arises between CR1 and CR2 and the demand for reasonable costs.

5.2.2 Requirements from wind farm operators

Similar to consumers, wind farm owners or operators have certain demands on the existing power system in order to be able to sell the wind power production:

- Wind power requirement 1 (WP1): similar to consumer appliances, wind farms require a certain voltage level at the connection point as wind turbines are usually designed to operate within a specific voltage range (e.g. nominal voltage _10 %). For the consumers, the requirements are rather homogeneous, since all consumers use the same type of equipment. For wind farms the requirements can sometimes be softened, since wind farms can be designed to handle different quality levels.
- Wind power requirement 2 (WP2): in addition, wind farm owners want to be able to sell their power production to the grid when wind power production is possible (i.e. when the wind speed is sufficient), otherwise, the production has to be spilled, which means that the wind farm owner loses possible financial income.
- Wind power requirement 3 (WP3): WP1 and WP2 also concern the reliability of the power system at the connection point of the wind farm.

There is always a trade-off between costs (i.e. low system costs) and reliability. The higher the reliability is, the higher the costs.

5.3 More Integration issues

The challenge that the integration of wind power poses is to meet CR1 and CR2 and WP1 and WP2 in an economically efficient way (i.e. CR3 and WP3), even in the case of significant wind power penetration in the system [3]. This challenge will now be discussed in more detail using the simplified power system in Figure 5.1.

5.3.1 Customer requirement 1: voltage level at the connection point of the consumer

First we will assume that no wind power is installed in the power system shown in figure 5.1 and that the voltage U_o is kept constant by the generated power, $\mathrm{P_G}$. Now, the load $\mathrm{P_D}$ varies the currents I_3 and consequently $\mathrm{I_1}$ will vary. Hence, there will be a voltage drop over the corresponding impedances Z_3 and Z_1. If impedances Z_3 and Z_1 are large (e.g. in the case of long lines or a comparatively low voltage) voltage$\mathrm{U_3}$ will vary substantially when P_D varies. Possible measures to avoid large voltage variations in U_3, are as follows.

- Measure (a): use a stronger grid (i.e. impedances Z_3 and Z_1 are small). This is possible by using higher voltages in the lines and transformers that are not too small.
- Measure (b): control the voltage U_3 by using controllable transformers close to $\mathrm{U_3}$.
- Measure (c): control voltage U_1 by using controllable transformers and/or some voltage controlling equipment such as shunt capacitors and/or shunt reactors.

It will now be assumed that wind power, P_w, is connected to the power system in figure 5.1. As the wind power production $\mathrm{P_w}$ will vary, current I_2 varies. Hence, current I_1 will vary, which will cause a voltage drop in U_3furthermore, U_1 will vary and possibly also the voltage close to the customer connection point, voltageU_3. The impact of wind power variations on the voltage variations in U_3 depends mainly on the size of impedanceZ_1. On the other hand, if Z_1 is large, there will be a strong connection between wind power variations and voltage variations in U_3. However, if Z_1 is very small, voltage U_3 will be more or less independent of wind power variations. In reality, only consumers that are rather close to wind farms may be affected by variations in wind power production. To avoid problems for consumers close to wind turbines, Measures (a)‑(c) can be used as well as the following measure:

- Measure (d): use local control of voltage U_2 at the wind farm. Depending on the wind turbine technology, the voltage control of U_2 can be performed by the wind.

5.3.2 Wind power requirement 1: voltage level at connection point of the wind farm

The voltage U_2 will also depend on P_w, P_D and the size of Z_3 and Z_2. The difference to the previous discussion on CR1 is that the size of Z_2 is important instead of the size of Z_3. This is mainly of interest when wind power is located at a larger distance from the consumers. In this situation, Measures (a), (b) and (d) explained above are of a certain interest as well as the following:

- Measures (e): use a controllable transformer close to U_2. A controllable transformer is normally slower than application of Measure (d), though.

5.3.3 Customer requirement2: power availability on Demand and Frequency Issues

Again, we will first assume that there is no wind power connected to the power system shown figure 5.1. Hence, when consumers increase their consumption, the power will be delivered directly from the conventional power plants [2].

Conventional power plants generally use synchronous generators which can be modelled as shown in figure 5.2. The figure includes the generator and the steam or hydro turbine. The turbine rotates and drives the rotor of the generator. $\mathrm{P_T}$ is the power delivered by the turbine and P_s is the power delivered from kinetic energy stored in the rotating mass consisting of turbine, shaft and rotor. During normal operation P_s is *0.* P_G is the electric power delivered to the power system.

If the load $\mathrm{P_D}$ increases, the power generation, P_G, will directly increase. However, the initial increase in power production is not due to an increase in the power production in the steam or hydro turbine. The increase of P_G will originate from the stored kinetic energy,P_s. Since the kinetic energy is used, the turbine–shaft–generator rotational system will slow down. Now, as the rotor speed of a synchronous generator is strongly coupled to the power system frequency, a decrease in rotor speed will result in a decrease in electric frequency. Therefore, a load increase will lead to a decrease in electric frequency.

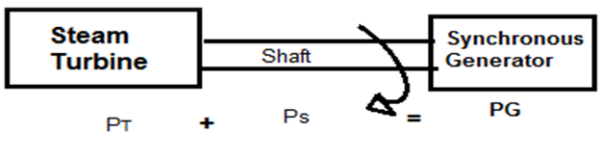

Figure 5.2. The Power balance in a conventional power plant

In order to limit the decrease in power system frequency, some power plants are equipped with a so-called primary control system [4]. This system measures the power system frequency and adjusts the power production of the power plant (i.e.P_T) when the frequency changes. The reaction time of primary control units depends on the power plants (e.g. how fast the production of steam can be increased).

Usually, primary control units can increase their production by a few percent of rated capacity within 30 seconds to 1 minute. Secondary control (i.e. power plants with a slower response), will take over the capacity tasks of the primary control 10 to 30 minutes later and will thereby free up capacity that is used for primary control. The requirement of load balancing (i.e. so that consumers' demand for power can be met) means that:

- power system must have sufficient primary and secondary control capacity available in order to be able to respond to changes in demand;
- these power plants must always have sufficient reserve margins to increase the power production to the level required for always meeting the system demand (i.e. the aggregated consumer demand).

If WECS is added to such a power system, there will be an additional fluctuating source in the power system. Depending on the system design and load characteristics, with increasing wind power penetration, the requirements regarding power system balancing may increase [5]. However, the primary and secondary control system will operate in exactly the same way as described above. Also, if wind power production decreases this has exactly the same effect on the system as an increase in demand according to Equation 5.1.

The consequence is that there will be more variations that have to be balanced by primary and secondary control. Experiences show that, even very high wind power penetration levels (up to 20 %), may not require additional primary control capacity as long as the installed wind power capacity is geographically distributed over a wide area [5].

The smoothing effect related to geographical distribution will result in low short-term variations in wind power production. However, owing to current limitations in wind speed forecast technologies, any mismatch between forecasted wind power production and actual wind power production has eventually to be handled by the secondary control capacity [4][5]. The requirements for secondary control capacity are therefore significantly influenced by the wind power penetration level. The additional system requirements for keeping the system balanced at all times depends very much on the individual system; that is, it depends on the load characteristics, the flexibility

of the existing conventional power plants and the wind power penetration as well as the geographic distribution of the wind farms. The cost of meeting the increased requirements depends on the type of power plant (i.e. PG), the size of interconnections to neighboring systems and, of course, on the additional requirements.

5.4 Network availability and power system reliability

5.4.1 Stability and reliability Issues

However, the introduction of wind power modifies the economic trade-off between reliability costs and consumer costs for insufficient reliability. Some of the trade-offs apply only to wind farms (i.e. they affect income for wind farm owners, but not consumers) and some affect the whole system.

An important reliability issue is related to the capacity margin in a given power system (i.e. there must be enough capacity available in a power system to cover the peak load). If we assume a certain power system, there is always a probability that the available power plants are not sufficient to cover the peak load. If WECS is added to a power system, reliability will increase as there is a certain probability that there will be a certain amount of wind power production available during a peak load situation, which will decrease the risk of capacity deficit. Adding more wind power capacity to a power system may also allow a decrease in the installed capacity of other power plants in the system without reducing the system reliability. In addition, depending on the power system design and the wind power penetration, power system reliability might be affected by the introduction of wind power because of the influence it has on stability in the case of a fault in the power system [2].

It should also be considered that, in contrast to systems with only varying load, active power balancing in a system with both wind power and load varying may require more balancing equipment to keep a certain system reliability level, since the total variation may increase. However, the cost–benefit analysis should consider that, for instance, the largest possible decrease in wind power (which requires an increased production from other power plants) can coincide with high wind power production. In such a situation, other power plants may have previously reduced their power production as a result of increasing wind power production. Hence, these (conventional) power plants may be able to increase production if wind power production decreases. Also, in this case the trade-off between the consumer benefit of high reliability and system costs for back-up and reserves have to be taken into account. An important issue here is, for instance, how fast aggregated wind power production can decrease during times when aggregated load levels typically increase very fast.

Now, suppose the reliability issues related to the installation of a certain wind farm is considered. Then, the dimensioning of the transmission system between the wind farm and the rest of the grid has to be discussed. Starting with the assumption that good wind resources are located in remote areas, at a larger distance from the rest of the power system a back-up transmission system between the wind farm and the main grid will be rather expensive compared with the economic benefits a back-up transmission system may. Hence the lack of a redundant transmission line may have a negative impact on the technical availability of wind farms. In this case, the compromise must consider the costs of a redundant transmission system and the lost income for wind farm owners during times when the transmission system is interrupted. Furthermore, the required power quality level at the connection point of the wind farm might be of importance. If very stable voltage level and frequency level are required, the grid has to incorporate some voltage regulating equipment end frequency controllers.

It must also be noted that the current variations from the wind farms will affect the voltage drop over Z_1. The most extreme cases occur during times with maximum wind power production (P_w) and minimum consumption (P_D), and zero wind power production (P_w) and maximum consumption (P_D). This implies that U_1 will show increased variation with increasing installed wind power, which may require additional voltage control equipment. However, it might be important to consider the probability of those extreme cases. The probability of full production in all wind farms at the same time that the load is at its minimum, for instance, might be low, so that additional voltage control equipment will not be required. The question is, for how severe situations should the voltage control equipment be designed? It is not economically relevant for all points within a network to keep a voltage within certain limits 100% of the time.

5.4.2 Frequency control Issues

In the power system, the frequency is an indicator of the balance or imbalance between production and consumption. For normal power system operation, the frequency should be close to its nominal value. In the case of an imbalance between production and consumption, primary and secondary control is used to return to a balanced system. If, for instance, consumption is larger than production, the rotational energy stored in large synchronous machines is utilized to keep the balance between production and consumption and, as a result, the rotational speeds of the generators decrease. This results in a decrease of the system frequency. In a power system, there are some units that have frequency-sensitive equipment.

These units are called primary control units. The primary control units will increase their generation until the balance between production and consumption is restored and frequency has stabilized. The time span for this control is 1–30s. In order to restore the frequency to its nominal value and release used primary reserves, the secondary control is employed with a time span of 10–15 min [2]. The secondary control thus results in a slower increase or decrease of generation. In some countries, automatic generation control is used; in other countries the secondary control is accomplished manually by request from the system operator.

At normal operation, the power output of a wind farm can vary up to 15% of installed capacity within 15 minutes. This could lead to additional imbalances between production and consumption in the system. Considerably larger variations of power production may occur during and after extreme wind conditions.

As wind turbines use other generation technologies than conventional power plants, they have a limited capability of participating in primary frequency control in the same way conventional generators do. However certain systems requires wind farms to include primary frequency control capabilities of 3–5 %(as required for thermal power plants) into the control of wind farm power output. Such systems and some other regulations also require wind farms to be able to participate in secondary frequency control. During over frequencies, this can be achieved by shutting down of some turbines in the wind farm or by pitch control. Since wind cannot be controlled, power production at normal frequency would be intentionally kept lower than possible in order for the wind farm to be able to provide secondary control at under frequencies. In the case of large frequency transients after system faults, regulation requires the wind farm to contribute to frequency control (i.e. secondary control).

5.5 Summary

This chapter provided an overview of the challenges regarding the integration of wind power into power systems. The overall aim of power system operation, independent of wind power penetration levels, is to supply an acceptable voltage and power to consumers and continuously to balance production and consumption. However, in so doing, the frequency should be kept within pre-specify limits. Furthermore, the power system should have an acceptable reliability level, with or without wind power penetration. Therefore, this chapter has discussed the impact of wind power on voltage and frequency control and overall system balance. The chapter discusses the basics of how wind power production behaves in order to arrive at a better understanding of integration issues.

5.6 References

[1] T. Sun, Z. Chen, F. Blaabjerg, “Voltage Recovery of Grid-Connected Wind Turbines with DFIG After a Short-circuit Fault”, 35th Annual lEEE Power Electronics Specialists Conference, Aachen, Germany, 2004

[2]Thomas Ackermann, Wind Power in Power Systems, john wiley and sons. Copyright 2005

[3] Li LIN, Yan ZHANG, Yihan YANG, Transient Characteristics of the Grid-connected Wind Power Farm with DFIGs and SCIGs, DRPT2008 6-9 April 2008 Nanjing China

[4]Anca D. Hansen et al, Centralised power control of wind farm with doubly fed induction generators, Renewable Energy Journal, Renewable Energy 31 (2006) 935–951, Science Direct

[5] Johan Morren, Sjoerd W. H. de Haan, Wil L. Kling, and J. A. Ferreira, Wind Turbines Emulating Inertia and Supporting Primary Frequency Control , IEEE Transaction on Power Systems, Vol. 21, NO. 1, February 2006

[6] Zehnder and Warhaft, Alan and Zellman. "University Collaboration on Wind Energy". Cornell University. Retrieved 17 August 2011.

Chapter 6

Smoothing Output Fluctuations in Power Systems with Wind Farms by Using Coefficient Diagram Method

6.1 Introduction

From Chapter 5, it is clear that wind farms integration may lead to reliability problems in power system [1]. This is because the wind is unstable, and since the wind is unstable, the output of wind generators may cause the output of the power system to become unstable [2]. Several problems may actually arise, one of which is network frequency variation. This is a serious problem that can affect the power quality. Therefore a control system is required in order to smooth the fluctuations caused by wind farm integration. This chapter is concern with implementing the proposed CDM as a control technique for smoothing of output fluctuations caused by wind farm integration.

6.2 SYSTEM CONFIGURATION

In this section, a simplified frequency response model for a single area power system with an aggregated generator unit is described [3].

6.2.1 System Dynamics

The overall generator–load dynamic relationship between the incremental mismatch power $\Delta P_m - \Delta P_L$ and the frequency deviation Δf can be expressed as:

$$s.\Delta f = \left(\frac{1}{2H}\right).\Delta P_m - \left(\frac{1}{2H}\right).\Delta P_L - \left(\frac{D}{2H}\right).\Delta f \qquad (6.1)$$

while the dynamics of the governor can be expressed as:

$$s.\Delta P_m = \left(\frac{1}{T_t}\right).\Delta P_g - \left(\frac{1}{T_t}\right).\Delta P_m \qquad (6.2)$$

and the dynamics of the turbine can be expressed as:

$$s.\Delta P_g = \left(\frac{1}{T_g}\right).\Delta P_c - \left(\frac{1}{R.T_g}\right).\Delta f - \left(\frac{1}{T_g}\right).\Delta P_g \qquad (6.3)$$

The block diagrams of the past equations are included in figure 6.1 where ΔP_g is change in the governor output, ΔP_m is change in mechanical power, Δf is frequency deviation, ΔP_L is the load change, ΔP_c is the supplementary control action, H is the equivalent inertial constant, D equivalent damping coefficient, R is speed drop characteristics, while T_g and T_t are governor and turbine time constant respectively.

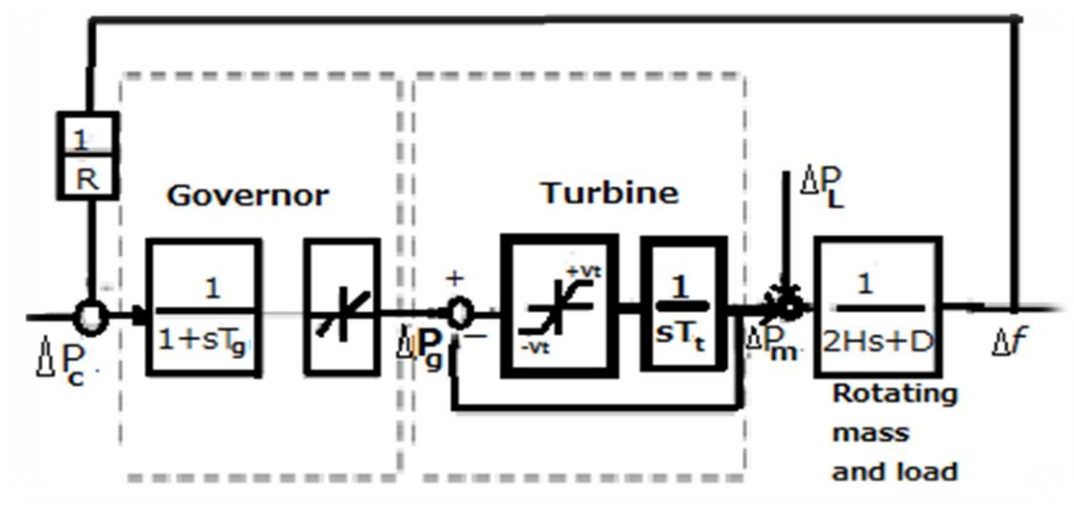

Figure 6.1. Block diagram of the single area power system

6.2.1.1System Dynamics:Simplified Wind Turbine Model for Frequency Studies

A simplified model of DFIG based wind turbine (WT) for frequency response [4] is shown in figure 3. This simplified model can be described by

$$si_{qr} = -\left(\frac{1}{T_1}\right).i_{qr} + \left(\frac{X_2}{T_1}\right).V_{qr} \qquad (6.4)$$

$$s.\omega = -\left(\frac{X_3}{2H_t}\right).i_{qr} + \left(\frac{X_2}{2H_t}\right).T_m \qquad (6.5)$$

$$P_e = \omega.X_3.i_{qr} \qquad (6.6)$$

For linearization, equation (6.6) can be rewritten as:

$$P_e = \omega_{opt}.X_3.i_{qr} \qquad (6.7)$$

where ω_{opt} is the operating point of the rotational speed, S is the differential operator, T_e is the electromagnetic torque, T_m is the mechanical power change, ω is the rotational speed, P_e is the active power of wind turbine, i_{qr} is q-axis component of the rotor current, V_{qr} is q-axis component of the rotor voltage and H_t is the equivalent

inertia constant of wind turbine. Table 6.1 shows the detailed expressions of the main parameters utilized for the simplified model of figure 6.2.

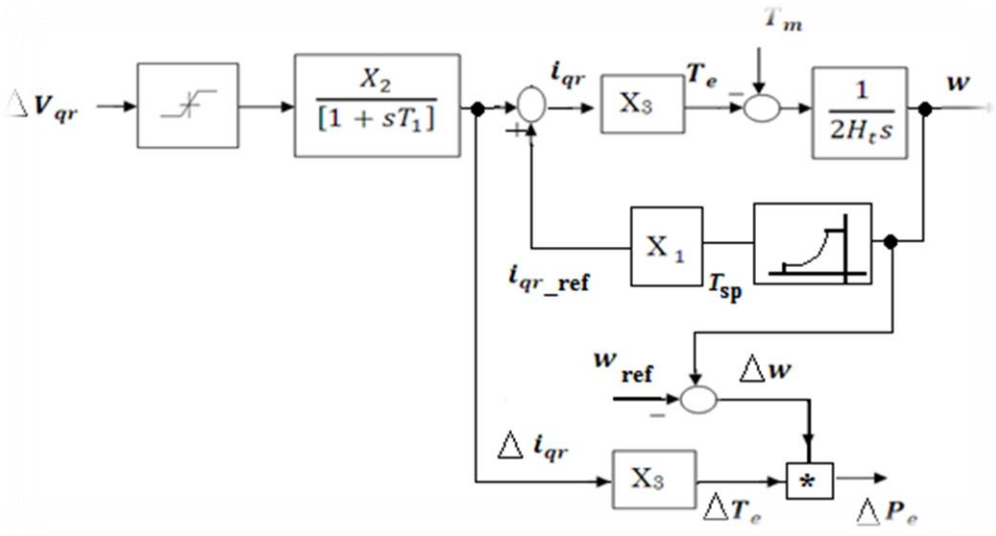

Figure 6.2. Simplified model of DFIG based wind turbine [5]

The parameters for the model shown in figure 6.2 are shown in table 6.1. below

Table 6.1 Parameters of figure 6.1 [6]

X_2	X_3	T_1
$\frac{1}{R_T}$	$\frac{L_m}{L_{ss}}$	$\frac{L_0}{\omega_s R_s}$

Where:

$L_0 = L_{rr} + \frac{{L_m}^2}{L_{ss}}$, $L_{ss} = L_s + L_m$ and $L_{rr} = L_{rs} + L_m$.

ω_s is synchronous speed, L_m is the magnetizing inductance, R_r and R_s are the respective rotor and stator resistances, L_r and L_s are the rotor and stator leakage inductances respectively, while L_{rr} and L_{ss} are the rotor and stator self-inductances.

6.3 OVERALL STEM STRUCTURE

The block diagram of a simplified frequency response model of a single area power system with aggregated unit including the proposed CDM controller is shown in figure 6.3.

The system consists of the rotating mass and load, nonlinear turbine with GRC, and governor with dead-band constraint [7].

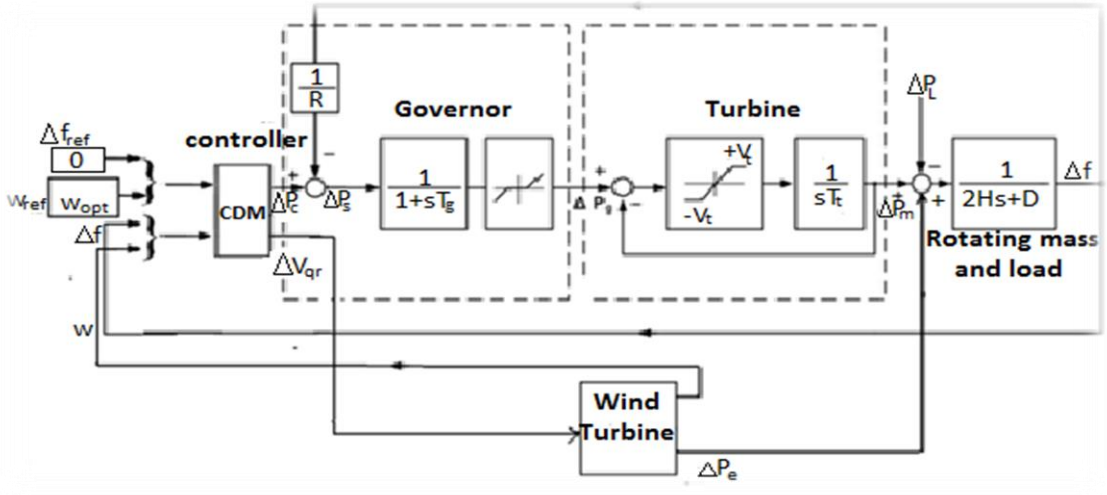

Figure 6.3. Block diagram of a single area power system with the proposed CDM controller

The frequency deviation is used as feedback for the closed loop control system. The measured and reference frequency deviation Δf and the reference frequency $(\Delta f_{ref} = 0\ Hz)$ are fed to the CDM in order to obtain the supplementary control action, ΔP_c, which add to the negative frequency feedback signal. The resulting signal ΔP_s is fed the governor giving the governor valve position which supplies the turbine to give the mechanical power change, ΔP_m, which is affected by the load change, ΔP_L, giving the input to the rotating mass and load block in order to provide actual frequency deviation Δf.

6.4. RESULTS AND DISCUSSION

Computer simulations have been carried out in order to validate the effectiveness of the proposed scheme. The Matlab/Simulink software package has been used for this purpose. A practical single area power system has the following nominal parameters [3] listed below in table 6.2.

Table 6.2 Parameters and data of pratical single area power system

D(p.u/Hz)	H(pu.sec)	R(Hz/p.u)	T_g(sec)	T_t(sec)
0.015	0.08335	3.00	0.08	0.4

Simulation studies are carried out for the proposed controller with generation rate constraint (GRC) of 10% p.u. per minute. The maximum value of dead band for governor is specified as 0.05%. The parameters of the CDM controller are set as follows:

The time constant can be taken as $\tau = 2sec$. Hence, from (11)

$$P_{tareget} = 1 + 2S + 1.6S^2 + 0.64S^3 + 0.128S^4 + 0.0128S^5$$

the stability indices (γ_i) are determined as:

$$\gamma_i = [2.5,2,1.25,5.12] \quad , i \in [1,4] \quad , \gamma_0 = \gamma_5 = \infty$$

And the stability limits $(\gamma_i{}^*)$ *are* $\gamma_i^* = [0.5,1.2,0.6953,0.8]$

with $, i \in [1,4]$ $k_0 = 1$, then

$B_i = 1 + 1.036S + S^2 , i \in [1,4]$

$$A_i = .008 + 2.77S + 2.4S^2 , i \in [1,4]$$

Tuning factor $\alpha = 0.5$

For the simulations studies, three cases are investigated. The first case is a nominal case where the power system operates under normal operating conditions. The second case the changed case where changes are made in the parameters of the power system so as to carry out robustness investigations and comparison is made between the controllers. In the third case, the effect of WT on the power system is investigated considering variable wind speed. Table 6.3 shows the parameters and operating points of the wind turbine.

The parameters of the MPC controller are set as follows:

Prediction horizon = 10 , Control horizon = 2, Weights on manipulated variables = 0 ,Weights on manipulated variable rates = 0.1 ,Weights on the output signals = 1 and Sampling interval = 0.0003 sec. Constraints imposed over the control action, and frequency deviation are as follows: Maximum(Max) control action = 0.25 pu, Minimum(Min) control action = 0.25 pu, Max. frequency deviation = 0.25 pu, and Min. frequency deviation = -0.25 pu.

Table 6.3 Wind Turbine Parameters and operating point

Operating Point(mw)	Wind speed(m/s)	Rotational speed(m/s)
247	11	1.17
R_r (pu)	R_s (pu)	X_{lr} (pu)
0.00552	0.00491	0.1
X_{ls} (pu)	X_m (pu)	H_t (pu)
0.09273	3.9654	4.5

X_m is the magnetizing reactance while X_{lr} and X_{ls} are the leakage reactance of the rotor and stator respectively.

6.4.1 Effect of Wind Turbines

In order to further validate the effectiveness of the proposed CDM, a single area power system in the presence of wind farm is considered. First the wind speed is constant. Then later variable wind speed is considered. Simulations are carried out to observe the effectiveness of the proposed controller which is being tested for several mismatches and fluctuations in wind speed. Details of the results are shown in the next sections below.

6.4.1.1 Constant Wind Speed

First, the proposed CDM technique was tested on the power system with the wind speed held constant. Then at t=30sec there is a sudden change in load and parameter uncertainties. Figure 6.4 illustrates the waveforms associated with this simulation. During this changed case, with the conventional PI controller, the system goes out of step.

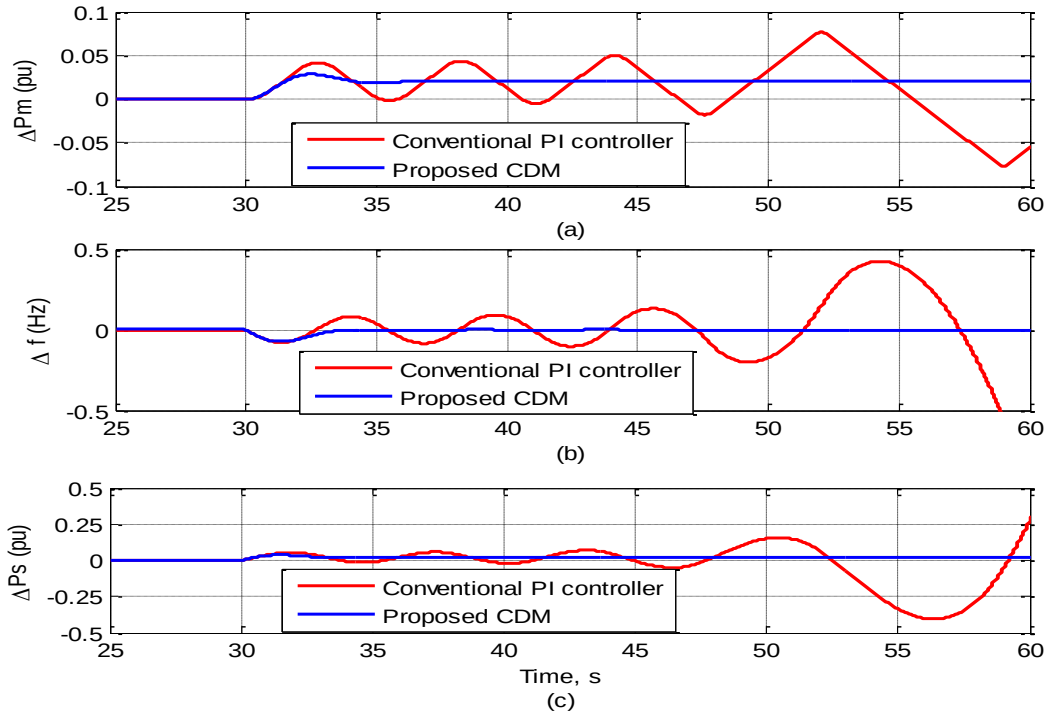

Figure 6.4. Power system response to different changes in the presence of Wind Farm during constant wind speed a) Mechanical power change, and b) frequency deviation

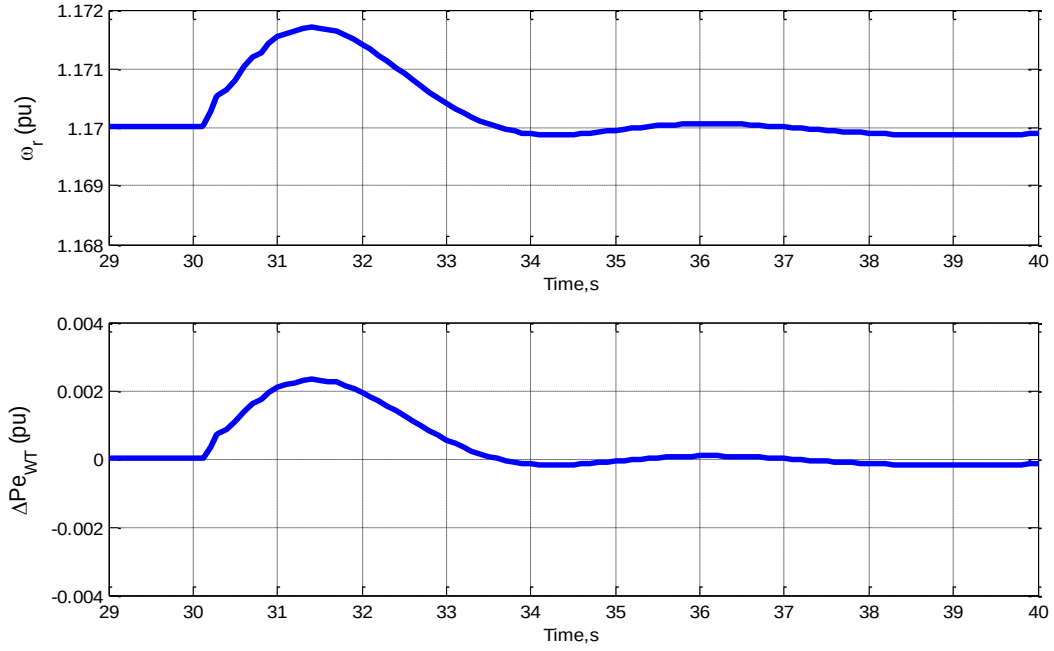

Figure6.5. Power system response to different changes in the presence of Wind Farm during constant wind speed a) rotational speed and b) WT electrical power output

However, figure 6.4 further shows that the power system operates effectively in the case where the proposed CDM technique is utilized. In figure 6.5 above, it can clearly be seen that the rotational speed of the WT tracks the power output of the as expected.

6.4.1.2 Variable Wind Speed

In order to further test the effectiveness of the proposed CDM control technique, simulation was performed and the system is observed in the presence of variable wind speed fluctuating between 7.5m/s to 15.5m/s as shown in figure 6.6 below.

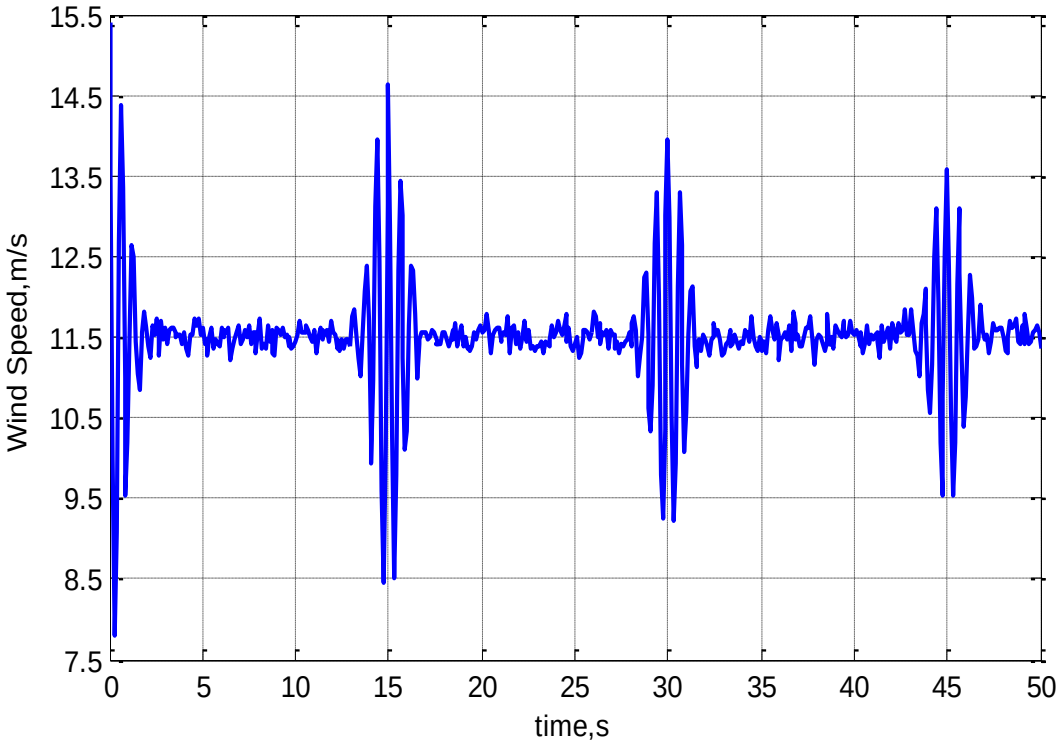

Figure 6.6. Simulated periodic wind speed fluctuation in m/s

Digital simulations are carried out in Matlab Simulink environment and the results are observed in figure 6.7. From the figure it can be seen that with the proposed strategy, the system is stable which verifies the effectiveness of the proposed control scheme. Here again, the power system with the proposed CDM exhibits the same response characteristics as that with the MPC.

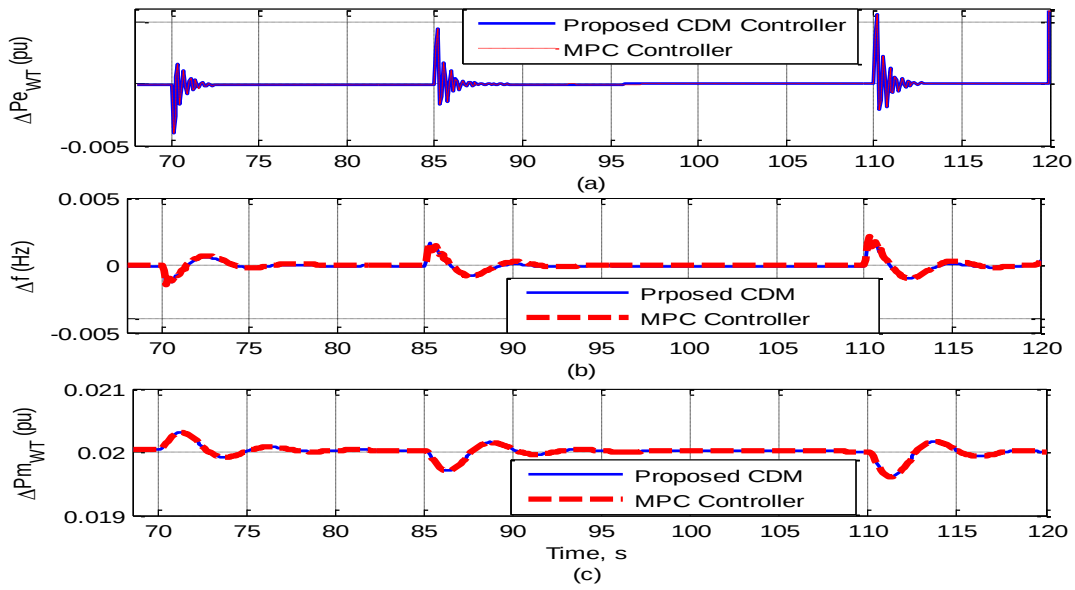

Figure 6.7. Power system response in the presence of Wind Farm with periodic wind speed fluctuations a) Wind Turbines electrical power output (b) frequency deviation and (c)mechanical power change

6.4.1.3 Wind Speed Fluctuation with Variable reference

Finally, a case is considered wherein the wind speed varies as well as its reference. In this case, figure 6.8 shows the wind fluctuating between 6m/s to 11m/s. According to the figure, the wind is initially fluctuating between 6m/s to 8m/s. Then at t=30s, a step change in wind speed occurs…the wind increases, and thus fluctuates between 8m/s and 11m/s.

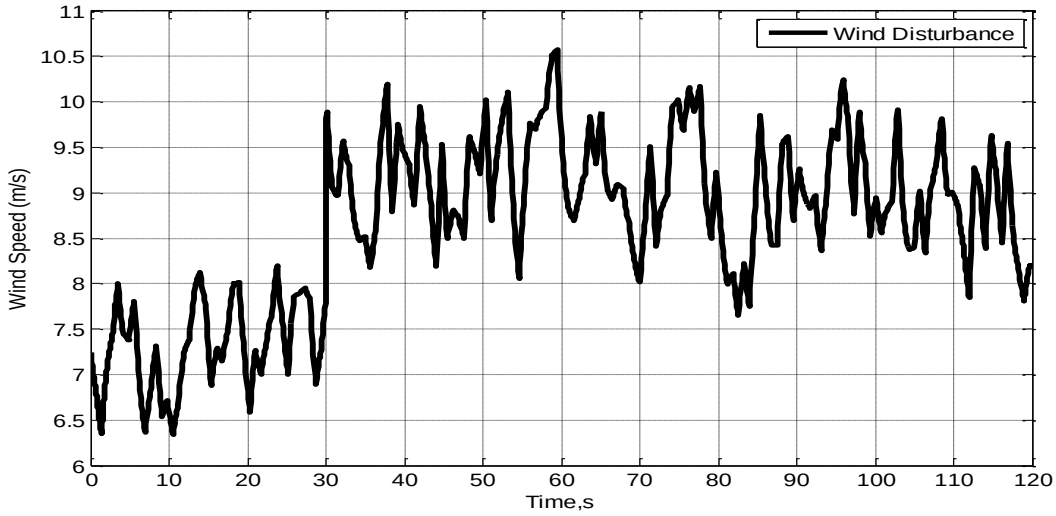

Figure 6.8. Changing-reference Variable wind speed

Simulation is carried out in the presence of the wind speed shown in figure 6.8 and then proposed CDM is implemented for power system frequency stability enhancement. Figure 6.9 shows the results of the simulation with the proposed CDM being compared to that of the MPC.

From the simulation result, the frequency deviation of the power system reaches about 0.0025Hz while the electrical power output deviation of the wind generators reaches 0.003pu maximum respectively in the case of both the proposed CDM and the MPC.

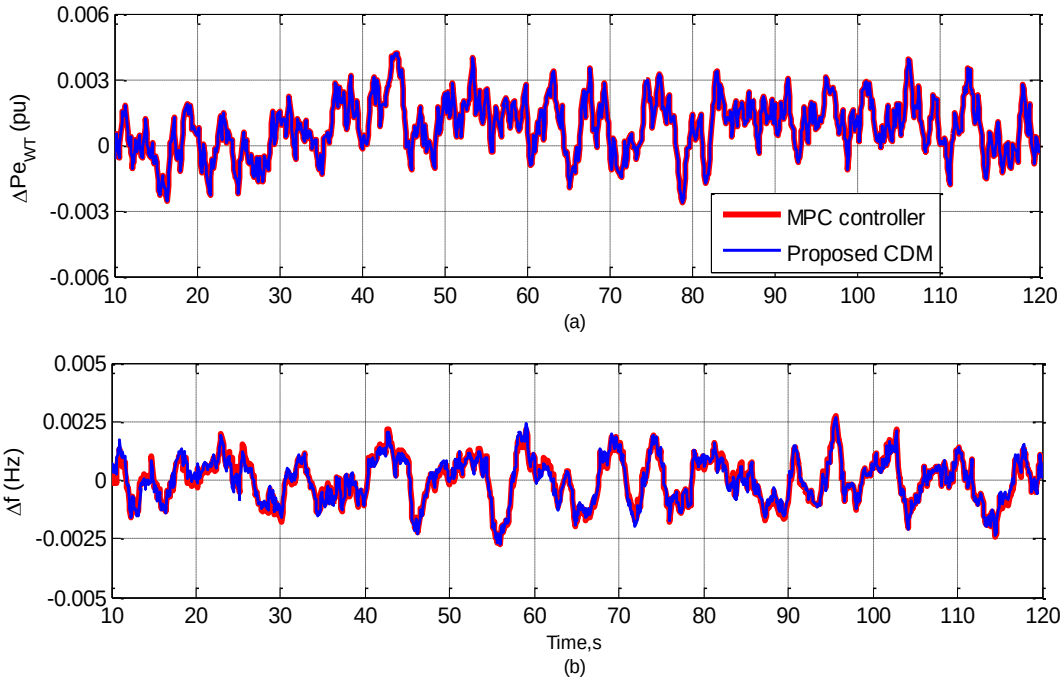

Figure 6.9. Power system response to Changing-reference Variable wind speed: a) Wind Turbines Electrical Power Output (b) Frequency deviation

As shown in figure 6.9, the response of the power system due to the implementation of both the proposed CDM and MPC are noticeably the same. It can be seen that with the proposed strategy, the system is stable which verifies the proposed technique can be applied basically not only to a generic power system, but also to system but also other types of power systems with renewable energy integration such as WES. Therefore the proposed method can contribute to expanding wind energy utilization; thus contributing to reducing greenhouse gas emission.

6.4.1.4 Proposed CDM Contribution to Reduction in Processing Time

In previous sections, it was stated that one of the most important advantages the proposed CDM is its simplicity which allows for reduction in procession time as compared to the MPC. To show this, simulation was carried out on the three area interconnected power system model utilized in chapter 4. When a model is simulated in Matlab and simulation is complete, then by using the Matlab command: tic;sim(gcs);toc, the elapsed real time or processing time in seconds is displayed in the MATLAB window.

Hence, in order to calculate the processing times for the CDM and MPC respectively, the same command was utilized using a fast computer with the following specifications shown in table 6.4.

Table 6.4 Specifications of the computer used to calculate controllers processing times

Windows Edition	Windows 7 Enterprise Service Pack 1
Processor	Intel®Core™i-7-4778 CPU
Frequency	3.40GHz
Installed Memory (RAM)	8.00(GB)
System Type	64-bit Operating System
Local Disc Space(HDD)	1TB (1000 GB)
Computer Name	michaelb-PC
Full Computer Name	michaelb-PC
Working Group	MITANILAB
Producted ID	55041-002-4356935-86910

The computer was issued to the author by Mitani laboratory, Kyushu Institute of Technology for research purposes. It should be noted that different computer specifications (especially speed) will lead to different results for the calculation. Figure 6.10 below shows the Matlab windows displaying the elapse time while using the MPC and the proposed CDM respectively.

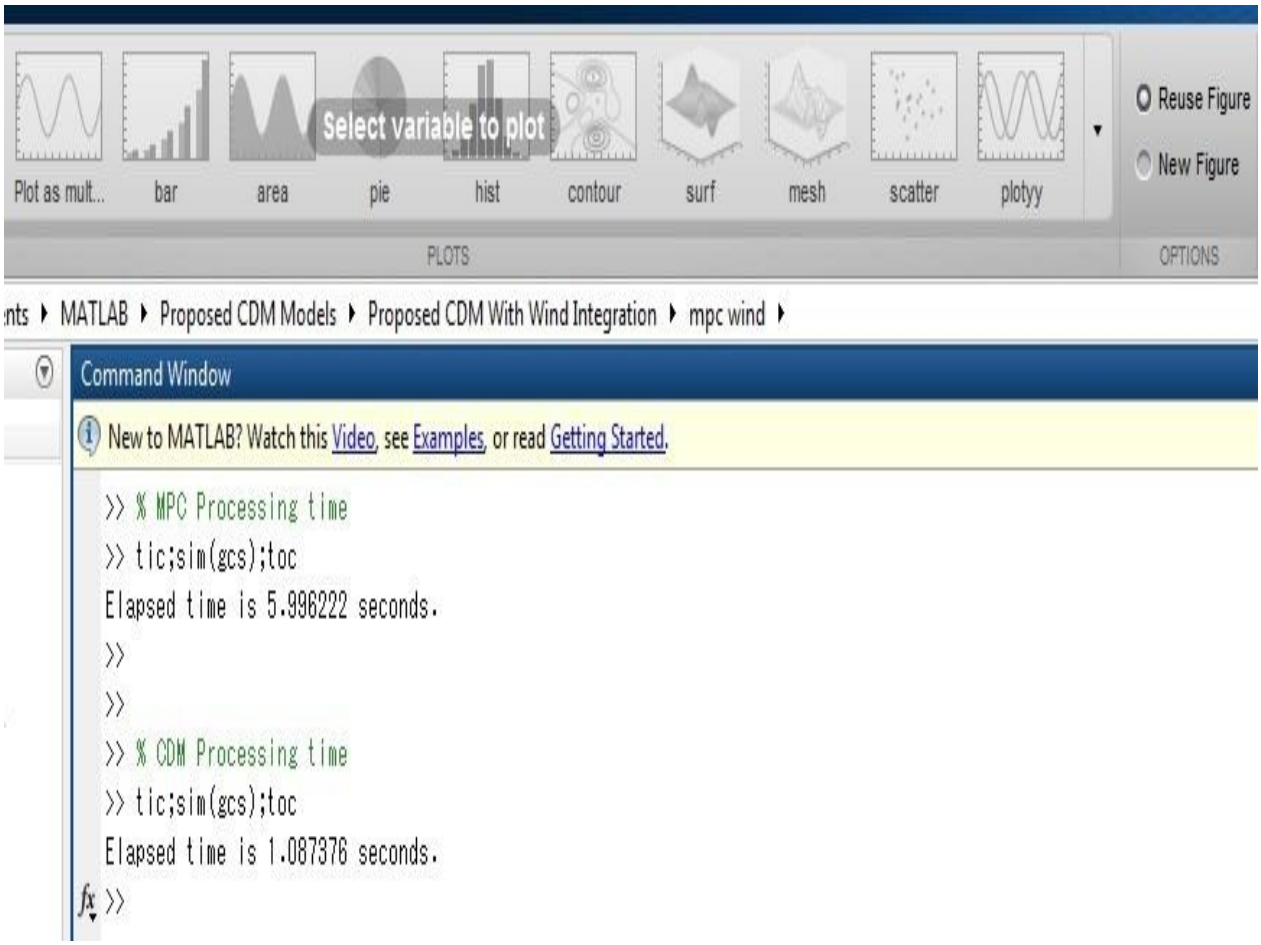

Figure 6.10. Matlab workspace showing calculated MPC and proposed CDM respective processing time

The real elapse times associated with both controllers are displayed in table 6.5 below.

Table 6.5 Case-1Real Processing Times for CDM and MPC

Controller	Simulation time	Real Processing time	Matlab version Used
MPC controller	120 seconds	5.996222 seconds	MATLAB R2014a
Proposed CDM	120 seconds	1.087376 seconds	MATLAB R2014a

According to table 6.5, the real time elapsed when implementing the proposed CDM controller is approximately five times than the time elapsed when implementing the MPC. This indicates that the proposed controller is less complex and reduces processing time five times as much as the MPC.

The same process was carried out considering a much smaller power system basically a single area power system, which was utilized in reference [8].

Table 6.6 Case-2 Real Processing Times for CDM and MPC

Controller	Simulation time	Real Processing time	Matlab version Used
MPC controller	120 seconds	1.659177 seconds	MATLAB R2014a
Proposed CDM	120 seconds	0.853285 seconds	MATLAB R2014a

In this case as shown in 6.6, the real time elapsed when implementing the proposed CDM controller is approximately twice the time elapsed when implementing the MPC. This indicates that when the complexity of the power system is increased, then, a significant enhancement in the processing time can be observed with the proposed controller as compared to the MPC.

6.4 Summary

This chapter investigates robust load frequency control of a single area power system in the presence of wind farm based on the proposed Coefficient Diagram method. Digital simulations have been carried out in order to validate the effectiveness of the proposed scheme. The proposed controller has been tested for several mismatched due to fluctuations in wind speed. First, simulations were carried out considering constant wind speed. Though the wind speed is constant, the power system undergoes disturbance such as sudden change in load and parameter uncertainties. The performance of the proposed CDM was compared to that of the conventional PI controller and the MPC. Simulation results show that fast response, robustness against parameter uncertainties and load changes can be considered as some advantages of the proposed CDM controller. It is shown that the proposed CDM controller response is much more effective than that of the traditional PI controller response and is able to deal with both uncertainties in parameters and load changes more efficiently. Also, it was shown that both proposed CDM and MPC are robust, but proposed CDM has the advantage over MPC with respect to reduced calculation burden, easier to design as well as being simple and reliable. Finally, with respect to variable wind speed, it is observed that the proposed CDM is also effective in smoothing output fluctuations caused by integration of wind turbines.

6.6 References

[1]Thomas Ackermann, Wind Power in Power Systems, john wiley and sons. Copyright 2005

[2] Flywheel

[3] H. Bevrani, "Robust Power system control", Springer, New York, pp. 15-61, 2009.

[4] J. Morel, H. Bevrani, T. Ishii, and T. Hiyama, " A robust control approach for primary frequency regulation through variable speed wind turbines ", IEEJ trans. Pe, Vol. 130, No. 11, 2010, pp. 1002-1009.

[5] Abdel-Magid, Y. L. and Dawoud, M. M., "Genetic Algorithms Applications In Load Frequency Control", Genetic algorithms in engineering systems: innovations and applications, 12-14 September 1995, conference publications No. 414, IEE, 1995.

[6] Yaser Soliman Qudaih, Michael Bernard , Yasunori Mitani and T. H. Mohamed, Model Predictive Based Load Frequency Control Design in the Presence of DFIG Wind Turbine, Proceeding of the 2nd International Conference on Electric Power and Energy Conversion Systems (EPECS'11), Sharjah, UAE, Nov. 15-17, 2011

[7] P. Kundur, Power System Stability and Control. New York: McGraw-Hill, 1994,pp. 581-585.

[8] Michael Z. Bernard, T.H.Mohammed, Yasunori Mitani, Yaser Soliman Qudaih, "CDM Application in Power System as a Load Frequency Controller", Proceedings of the 13th annual Electrical Power and Energy Conference (EPEC 2013), Halifax, Nova Scotia, Canada, August 21-23,2013 (5-pages, USB Flash Drive

Chapter 7

Conclusion and Future Work

7.1 Conclusion

This thesis proposes a new CDM based decentralized robust frequency control design for electric power system. The proposed technique modifies the standard CDM by appropriately introducing feed forward and feedback compensators to compensate for deficient performances. Benefits of the proposed controller include ensuring stability of the closed loop power system by robust performance, simple and easy to design, and applicable to every power system including those with wind energy integration thereby promoting the expansion of renewable energy utilization; thus contributing to reduction of greenhouse gas emission. The proposed CDM was investigated considering various cases. Interconnected power systems assumed similar to the interconnections of three MRU countries, Liberia, Guinea and Sierra Leone were tested, considering different load change and parameters change cases. Also, a single area power system with wind farm was investigated to test the controller for smoothing of output fluctuations caused by renewable energy integration. The results were compared with the results of a conventional PI and model predictive controllers. Simulation results demonstrated the effectiveness of the proposed CDM methodology. It was shown that the power system with the proposed CDM controller is robust against load changes and parameters' perturbations and has more desirable performance as compared to classical PI control design, in all of the performed tested cases. Also, the simulation results indicated that both CDM and MPC controllers can give robust response verses load change and parameters uncertainties, but the proposed CDM is more practical in term of the calculation burdens which is available in the case of MPC. Finally, it was observed that the proposed CDM can also effectively smooth output fluctuations caused by wind farms, thus, contribution to environmentally friendly power system while effectively promoting reliable power distribution.

7.2 Future Work

Though the CDM is robust and simple, its parameters are obtained sometimes based on experience and/or sometimes by trial and error method just like classical controller. Of course, utilizing compensators for the proposed CDM helped solve the problem. But the parameters of the controller obtained may not be the best. Therefore, it is important to develop an algorithm using optimization techniques as a search method for obtaining the best CDM Controller parameters.

Also, since integration of the two large power systems lead to different stability behavior and Wide Area Monitoring Systems (WAMS) based on phasor measurement units (PMUs) can be applied for monitoring of large interconnected power systems,

then use of PMU to monitor an existing power system first, before carrying out real time offline or online implementation of the propose control strategy as well as smart grid application are also considered for future work.

List of Papers

International Conference Proceedings

1. Michael Bernard, Yasunori Mitani, Masayuki Watanabe,Yaser Soliman Qudaih, Dikpride Despa, “Analysis and Simulation of DFIG Wind Farm Connected to Power System”, Proceeding of the 17th International Conference on Electrical Engineering (ICEE2011), Hong Kong, 10-14 July 2011 (6-pages CDROM)

2. Dikpride Despa, Yasunori Mitani, Masayuki Watanabe, Michael Bernard, Yaser Soliman Qudaih, “PMU Based Monitoring and Estimation of Inter-area Oscillation Mode Using Artificial Neural Network”, Proceeding of the 17th International Conference on Electrical Engineering (ICEE2011) Hong Kong (6-pages CDROM)

3. Yaser Soliman Qudaih, Michael Bernard, Yasunori Mitani, T.H. Mohammed, “Model Predictive Based Load Frequency Control Design in the Presence of Wind Turbines”, Proceedings of the 2nd International Conference (EPECS 2011), Sharjah, UAE, November 15-17, 2011 (6-pages, CDROM)

4. Dikpride Despa, Yasunori Mitani, Masayuki Watanabe, Yaser Soliman Qudaih, Taro Fujita, Qing Liu, Michael Bernard, “PMU Based Monitoring and Estimation Power System Dynamic Stability Developed on 50-Hz Power System”, Proceedings of the IASTED-International Conference on Power and Energy System (AsiaPES 2012), Phuket, Thailand, April 2012 (8-pages, CDROM)

5. Michael Z. Bernard, T.H.Mohammed, Yasunori Mitani, Yaser Soliman Qudaih, “CDM Application in Power System as a Load Frequency Controller”, Proceedings of the 13th annual Electrical Power and Energy Conference (EPEC 2013), Halifax, Nova Scotia, Canada, August 21-23,2013 (5-pages, USB Flash Drive

6. Raheel Ali, Michael Bernard, Yaser Soliman Qudaih, and Yasunori Mitani, T.H. Mohammed “A New load frequency control approach Utilizing Electric Vehicles and Heat Pump Water Heaters in Smart Power Systems Using Coefficient Diagram Method” 16th International Middle East Power System Conference(MEPCON’ 14) Cairo, Egypt, December 23-25, 2014 (7-pages, paper accepted)

Technical Journals and Transactions

1. Michael Z. Bernard, T. H. Mohamed, Raheel Ali, Yasunori Mitani, Yaser Soliman Qudaih “PI-MPC Frequency Control of Power System in the Presence of DFIG Wind Turbines” Journal of Energy and Power Engineering, ISSN1934-8975, Volume 5,Number 9B, Pp 43-50, September 2013

2. Michael Z. Bernard, T.H.Mohammed, Yaser Soliman Qudaih, Yasunori Mitani “Decentralized Load Frequency Control in an Interconnected Power System Using Coefficient Diagram Method” International Journal of Electric Power and Energy Systems, Volume 63, Pp 43-50, December 2014

Biography of the Author

The author was born in Monrovia Liberia in 1979. He received his B.Sc. degree in Physics with Minor in Mathematics from the University of Liberia in 2007. In 2012, he graduated with a Master of Engineering (M.Eng) degree from Kyushu Institute of Technology (Kyutech). He is currently a Doctor of Engineering (D.Eng.) student sponsored by the Japanese Government (Monbusho scholarship) at MITANI Laboratory, Kyushu Institute of Technology. His research interest includes, wind and solar energies, smart grid, power system modeling, stability and control.